Statistical properties of turbulent flows

P.D. Mininni

NCAR, Boulder, CO

A. Alexakis (NCAR) and A. Pouquet (NCAR)

mininni@ucar.edu

Outline

- Turbulence and the Navier-Stokes equations.
- Isotropic and homogeneous turbulence: K41 theory.
- Direct numerical simulations vs. large eddy simulations ("*models*").
- Hydrodynamic simulations at large resolution.
- Intermittency and high order statistics.
- The energy transfer and triadic interactions.
- Helicity in hydrodynamic turbulence.
- Some results for conducting fluids.
- Subgrid scale models.

Alexakis, Mininni, & Pouquet, PRL **95**, 264503; arXiv:physics/0602148

Alexakis, Mininni, & Pouquet, PRE **72**, 046301 and 046302

Turbulence

A turbulent flow is a strongly nonlinear, dissipative system with an extremely large number of degrees of freedom. Turbulence is characterized by:

- Strong and impulsive events
- Wide range of strongly interacting scales
- Sensitivity to initial conditions (but stable statistical properties; universality?)
- Highly dissipative, statistically irreversible
- Strongly diffusive (enhanced transport)
- Non-gaussian statistics

Due to the large number of degrees of freedom, tools are more likely to be probabilistic than geometric (as oposed to low dimensional chaos).

Turbulence

Two approaches:

- A *statistical theory of turbulence*
- Statistics used to characterize general properties of small scale turbulent flows:
  – Scaling with Reynolds number (Landau-Hopf theory of turbulence)

    What is the limit of large Reynolds number?

    How do we extrapolate from simulations and experiments to geophysical flows?

  – Scaling with scales at constant (but large) Reynolds number (Kolmogorov theory of turbulence)

    Self-similarity

    Universality

    Are the properties of the small scales independent of the large scale flow?

Turbulence

"I soon understood that there was little hope of developing a pure, closed theory, and because of absence of such a theory the investigation must be based on hypotheses obtained on processing experimental data." (Kolmogorov)

Statistics used to process experimental data:

- First studies focused on mean quantities (velocity), energy spectrum, and probability density functions (PDFs).
- Then multi-point correlations were considered (high order correlation functions and structure functions).
- More recently, conditional statistics were introduced.
- A need for "structure dependent" statistical quantities, or a link between statistics and structural properties of turbulent flows became apparent.

The Navier-Stokes equations

- Momentum equation

$$\frac{\partial \mathbf{v}}{\partial t} + (\mathbf{v} \cdot \nabla)\mathbf{v} = -\nabla P + \nu \nabla^2 \mathbf{v} + \mathbf{F} \qquad \nabla \cdot \mathbf{v} = 0$$

- P is the pressure, $\mathbf{F}$ an external force, ν the kinematic viscosity, and $\mathbf{v}$ the velocity; incompressibility is assumed.

- Quadratic invariants ($\mathbf{F} = 0$, $\nu = 0$):

$$E = \int \mathbf{v}^2 \, \mathrm{d}^3 x$$

$$H = \int \mathbf{v} \cdot \boldsymbol{\omega} \, \mathrm{d}^3 x \qquad \boldsymbol{\omega} = \nabla \times \mathbf{v}$$

- Reynolds numbers:

$$Re = UL / \nu \qquad R_\lambda = U\lambda / \nu$$

where L is the integral scale and λ the Taylor scale.

The energy cascade

Starting from

$$\mathbf{v} = \begin{bmatrix} \sin(k_0 x)\cos(k_0 y)\cos(k_0 z) \\ -\cos(k_0 x)\sin(k_0 y)\cos(k_0 z) \\ 0 \end{bmatrix}$$

as initial condition, and replacing in the Navier-Stokes equation

$$\frac{\partial v_x}{\partial t} = \frac{k_0 \sin(2k_0 x)}{8}\left[\cos(2k_0 z) - \cos(2k_0 y)\right] - 3k_0^2 \nu \cos(k_0 x)\sin(k_0 y)\sin(k_0 z)$$
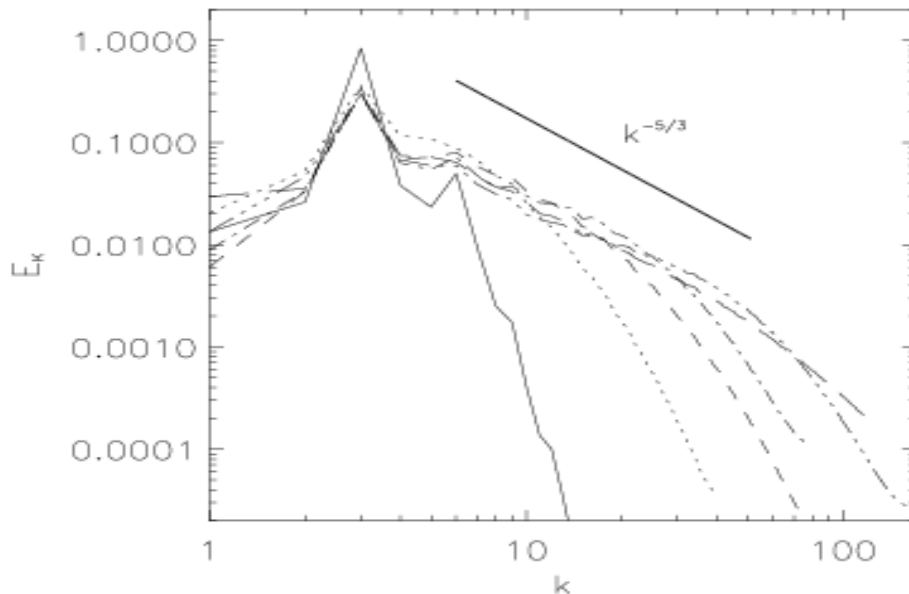
- This process can be repeated, and smaller eddies are created until reaching the scale where the dissipative term dominates! Taylor & Green, *Proc. Roy. Soc.* A **151**, 421 (1935)

Isotropic and homogeneous turbulence

- A uniform velocity field produces no distortion of small scale structures.

- Distortion is controlled by shear.

- Assuming predominant distortion comes from scales $l' \sim l$ (local interactions), for an eddy of size l distortion takes place in an inverse time $1/\tau_l = u_l/l$.

- The energy flux ε is constant in the inertial range. As a result, from the nonlinear term in the momentum equation $\varepsilon \sim u_l^2/\tau_l \sim u_l^3/l$, and $u_l^2 \sim l^{2/3}$.

- Then the energy spectrum is $E(k) = dE/dk \sim E/k \sim k^{-2/3}/k \sim k^{-5/3}$.
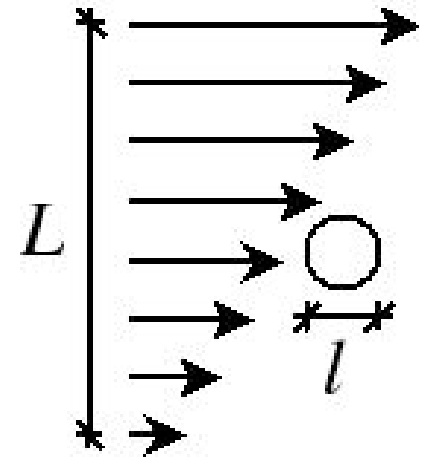
K41 and the dissipation scale

- Energy spectrum: $E(k) = C_k \, \varepsilon^{2/3} k^{-5/3}$
- Energy balance: from the Navier-Stokes equation

$$\mathrm{d}E/\mathrm{d}t = \varepsilon - 2\nu\Omega \qquad \text{where } \Omega = \int \omega^2 \, \mathrm{d}^3 x$$

- We can define a dissipation wavenumber as

$$\varepsilon = 2\nu \int k^2 E(k) \, dk$$
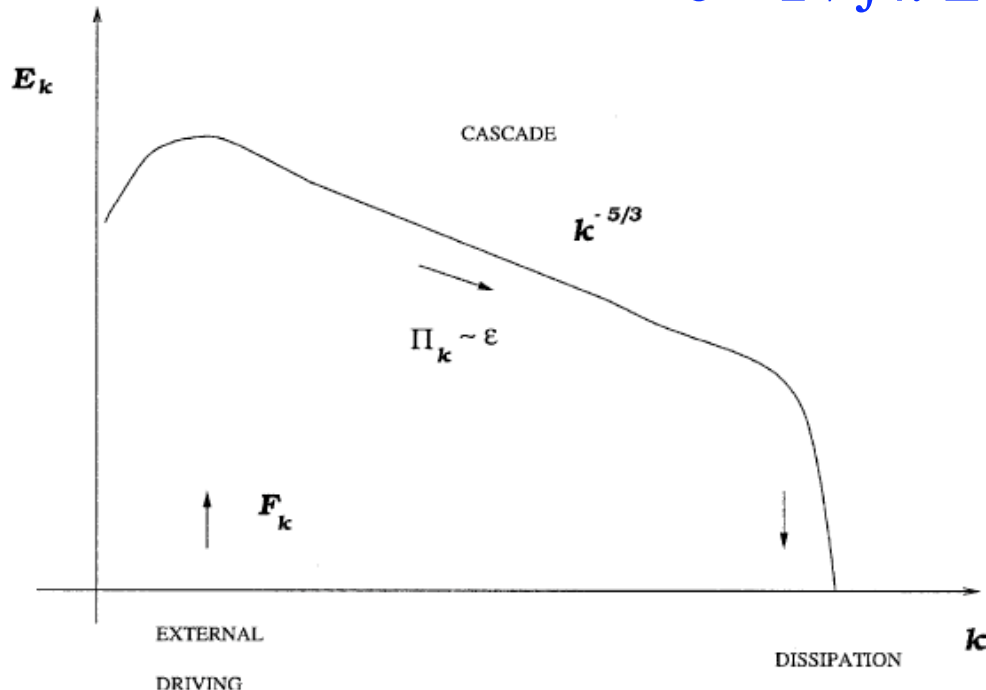
Then, $k_\nu = (\varepsilon/\nu^3)^{1/4}$ and $\eta = 2\pi/k_\nu$. The number of degrees of freedom goes as $N \sim (L/\eta)^3$. Using $\varepsilon = u_l^3/l$, then $N = Re^{9/4}$ (for the memory, time goes as Re^3)

E_k

CASCADE

$k^{-5/3}$

$\Pi_k \sim \varepsilon$

F_k

EXTERNAL

DRIVING

DISSIPATION

k

DNS: pseudospectral methods

- Given the dissipation scale (or the Reynolds number), a DNS (direct numerical simulation) satisfies $\eta > 2\Delta x$ (or $k_\nu < k_{max}$).
- No model or parametrization is used for the small scales, all the physical scales are resolved in the simulation: we learn about turbulence the hard way.
- In pseudospectral methods, we deal directly with spectral (Fourier) modes, which correspond to spatial scales.
- Periodic boundary conditions, Runge-Kutta in time, 2/3-rule for dealiasing.
- Quadratic ideal invariants are conserved in the truncated subspace.
- Exponential convergence.
- Conservative and non-dispersive.
- Spatial resolutions from 256^3 to 1024^3.
- Several forcing functions: Taylor-Green (TG), Arn'old-Beltrami-Childress (ABC), and random forcing (RND).

Pseudospectral method

- Burgers equation: $\partial_t u + u\partial_x u = v\partial_{xx} u$
- Projection into Fourier modes

$$u^N(x,t) = \sum_{k=-N/2}^{N/2} u_k(t)e^{ikx}$$

- We ask for the error projected in the subspace to be zero

$$\int e^{-ikx}(\partial_t - L)u^N \, dx = 0, \quad k = -N/2 + 1, \ldots, N/2$$

- Then we have a set of ODEs

$$\partial_t u_k = -(u\partial_x u)_k - vk^2 u_k, \quad (u\partial_x u)_k = \sum_{l+m=k} im u_l u_m$$

- The convolution needs N^2 operations (spectral method). Pseudospectral methods need *NlogN* operations.

Models: Reynolds averaged NS

- The flow is separated into mean and fluctuating components:

$$u(\mathbf{x}, t) = \bar{u}(\mathbf{x}) + u'(\mathbf{x}, t)$$

- Replacing in the Navier-Stokes equations, we obtain for the mean velocity field:

$$\frac{\partial \bar{u}_i}{\partial t} + \frac{\partial \bar{u}_j \bar{u}_i}{\partial x_j} = \bar{f}_i - \frac{1}{\rho} \frac{\partial \bar{p}}{\partial x_i} + \nu \frac{\partial^2 \bar{u}_i}{\partial x_j \partial x_j} - \frac{\partial \overline{u_i' u_j'}}{\partial x_j}$$

- The time evolution of the resolved field depends on the statistical properties of the unresolved scales (the closure problem).
- If these properties are in some sense "universal", from DNS we can learn how to parametrize the effect of the unresolved scales.

Models: Large eddy simulations

- The flow is separated into resolved and unresolved components:

$$u_i = \bar{u}_i + u'_i,$$

- Replacing in the Navier-Stokes equations, we obtain for the resolved velocity field:

$$\frac{\partial \bar{u}_i}{\partial t} + \bar{u}_j \frac{\partial \bar{u}_i}{\partial x_j} = -\frac{1}{\rho}\frac{\partial \bar{p}}{\partial x_i} + \frac{\partial}{\partial x_j}\left(\nu \frac{\partial \bar{u}_i}{\partial x_j}\right) + \frac{1}{\rho}\frac{\partial \tau_{ij}}{\partial x_j}.$$

- In theoretical approaches, ensembles are considered instead of time or spatial filters. In practice, how do we chose the filtering length?

- It is assumed that some form of an ergodic theorem holds for turbulent solutions of the Navier-Stokes equations.

A 1024^3 TG hydrodynamic simulation

$$\mathbf{F} = \begin{bmatrix} \sin(k_0 x)\cos(k_0 y)\cos(k_0 z) \\ -\cos(k_0 x)\sin(k_0 y)\cos(k_0 z) \\ 0 \end{bmatrix}$$

z
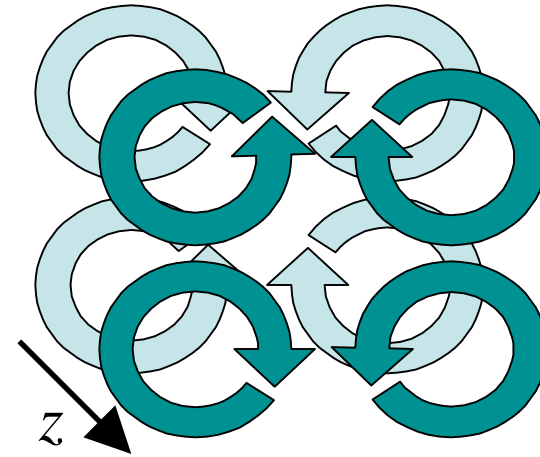
- Taylor-Green forcing.
- Non-helical force; helical fluctuations are generated locally by the nonlinear terms in the NS equation.
- Proposed as a paradigm of turbulence: eddies at the scale $1/k_0$ cascade down to smaller eddies until reaching the viscous scale. Taylor & Green, *Proc. Roy. Soc.* A **151**, 421 (1937)
- Another simulation with the same resolution using ABC forcing (helical force).

…and a 1024^3 ABC hydrodynamic simulation

$\mathbf{F} = [B \cos(k_0 y) + C \sin(k_0 z),$

$\quad A \sin(k_0 x) + C \cos(k_0 z),$

$\quad A \cos(k_0 x) + B \sin(k_0 z)]$
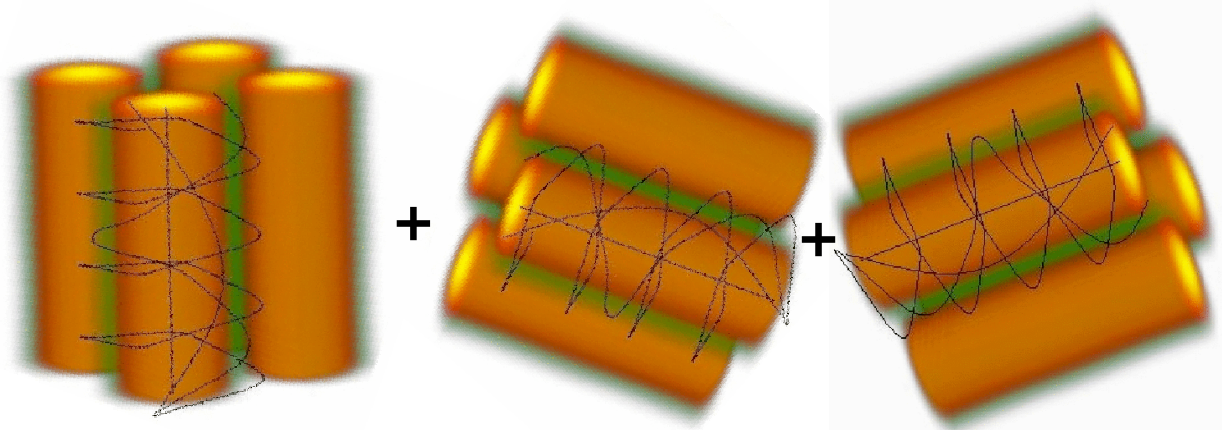
- Arn'old-Beltrami-Childress forcing.
- Helical force; the ABC flow is a Beltrami flow ($\nabla \times \mathbf{F} = k_0 \mathbf{F}$) and injects maximum helicity in the flow.
- It develops turbulence after a hydrodynamic instability.
- Proposed to study (fast) dynamo action.
- We also have simulations with random forcing to compare, although at smaller spatial resolution.

Large and small scale structures in TG

- 3D visualization of vorticity intensity in the tail of the PDF in the TG simulation.

- Turbulent fluctuations and a large scale pattern.

- High density of vortex tubes in regions with $\mathbf{F} = 0$.
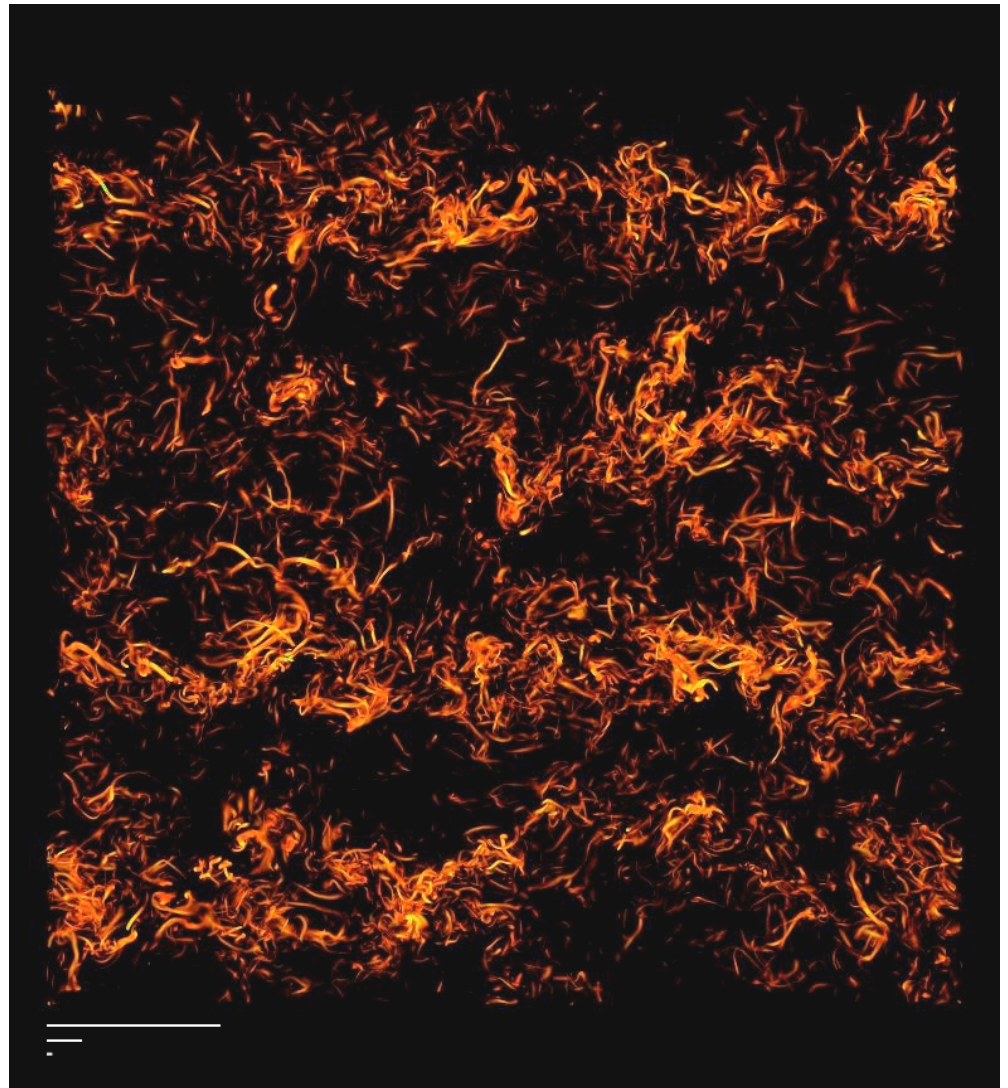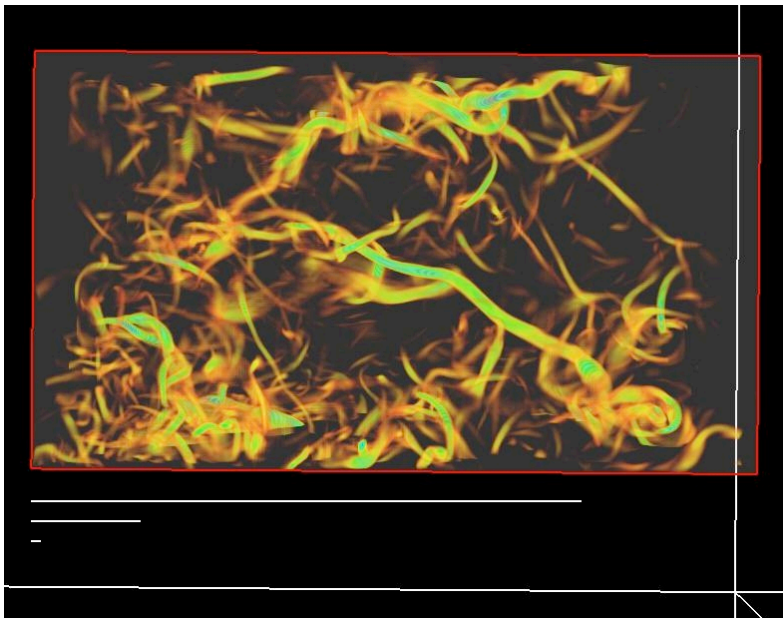
Large and small scale structures in ABC

- Again, patches can be observed.
- The geometry of the flow is complex
- Regions of strong and weak shear are more complex than in TG.
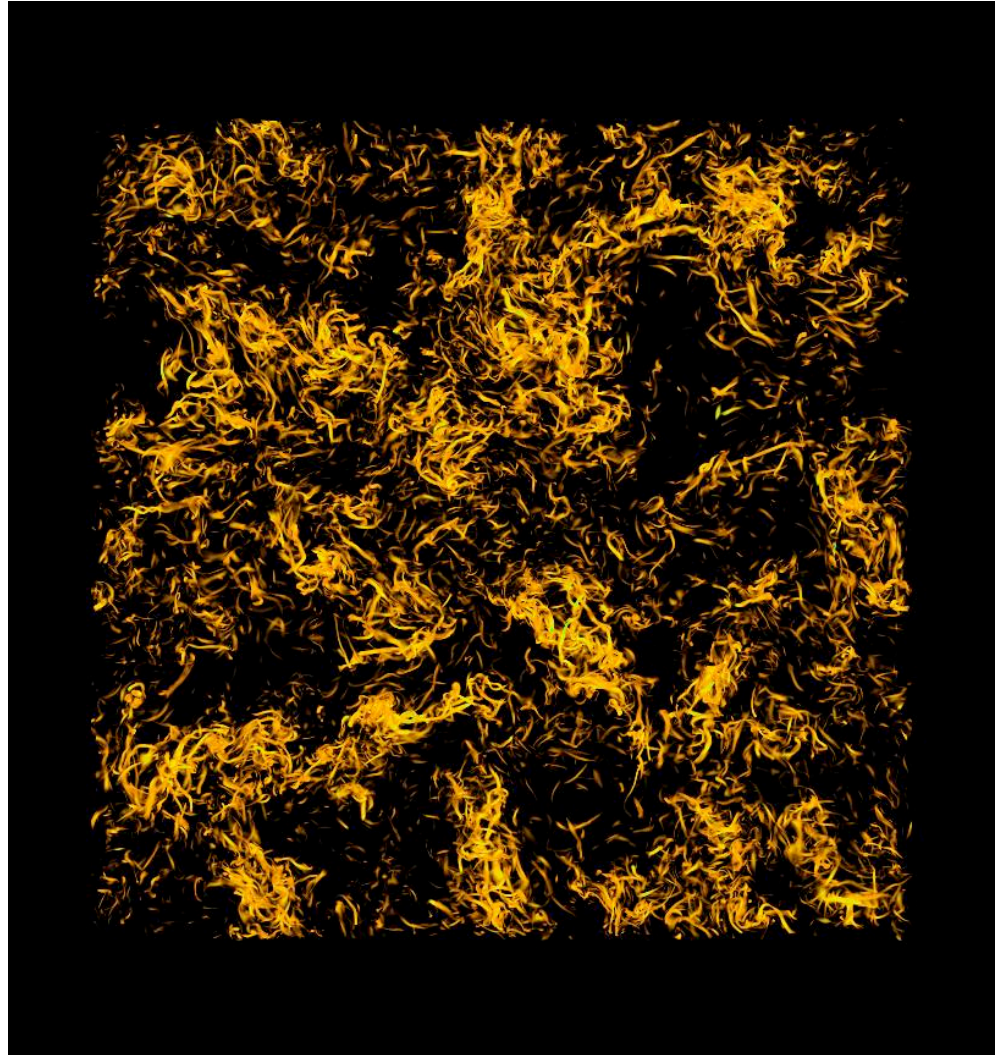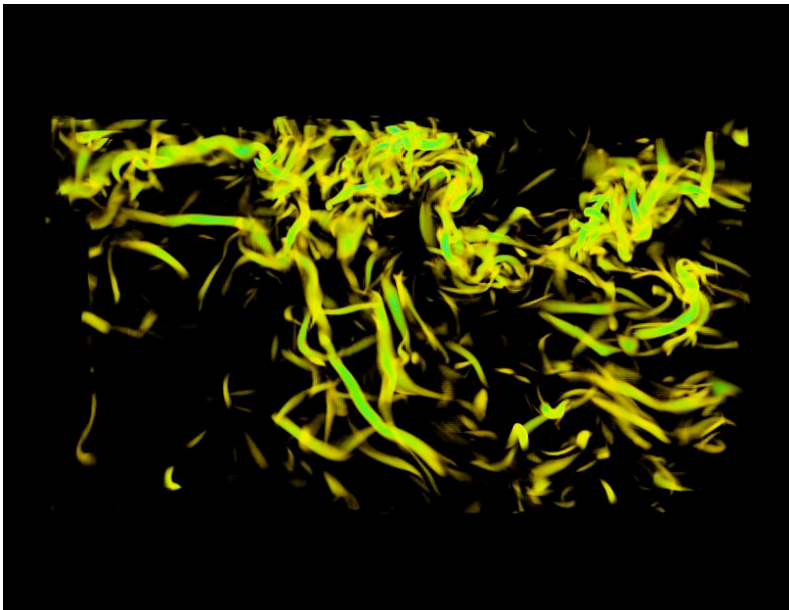
Vortex tubes
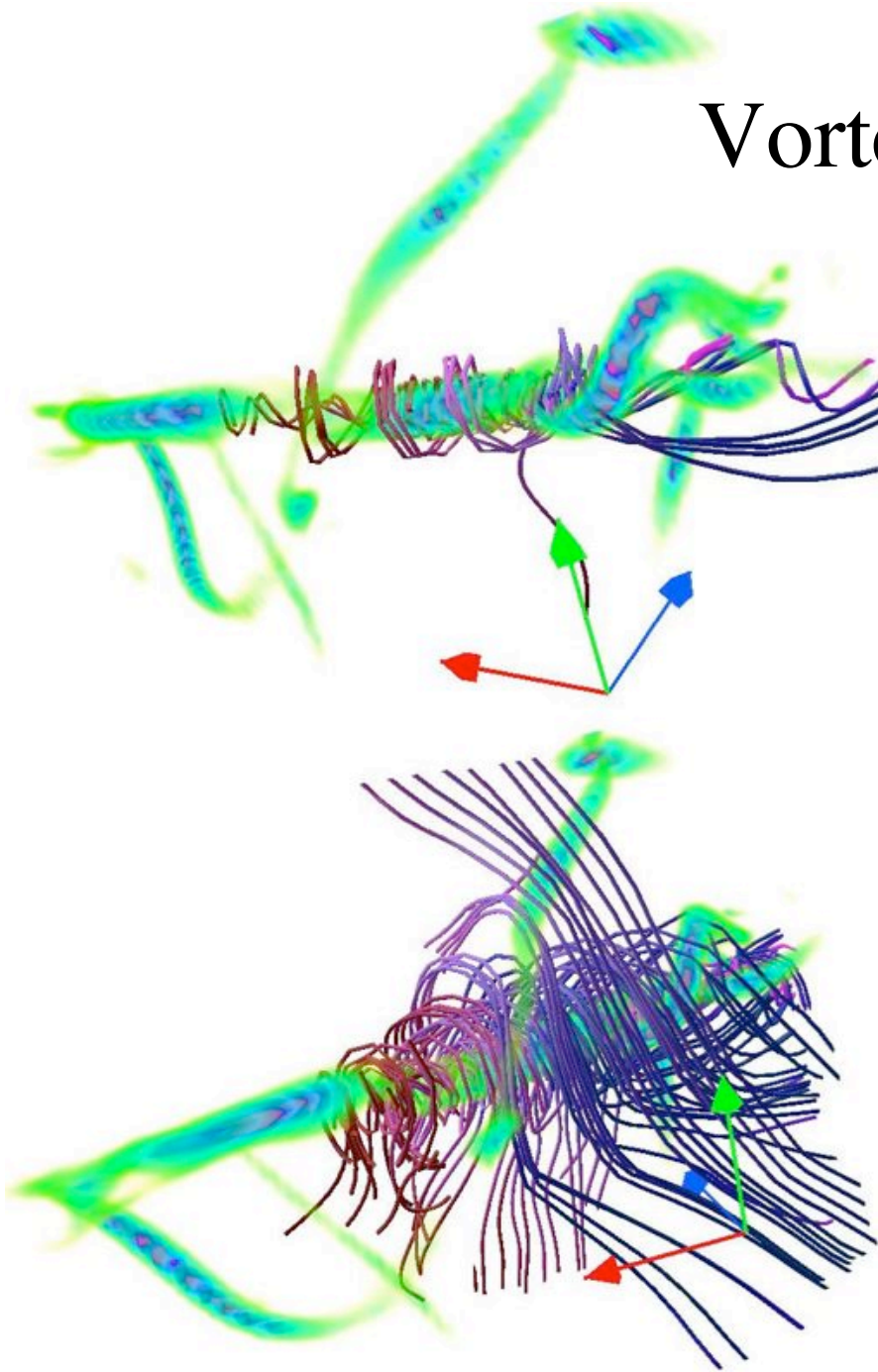
- 3D visualization of vorticity intensity in the tail of the PDF.
- Velocity field lines are shown inside and outside the structure
- The regions of strong vorticity correspond to vortex tubes.
- Elongated structures with a helical flow in the vicinity of the tube.
- Regions with parallel vorticity and velocity field are local exact solutions of the Navier-Stokes equations.

3D renders using VAPoR
(www.vapor.ucar.edu)

Large and small scale structures (TG)

- Relative helicity $h = \mathbf{v} \cdot \boldsymbol{\omega} / \langle |\mathbf{v}||\boldsymbol{\omega}| \rangle$ and vorticity intensity.

- Local beltramization. Tsinober & Levich, Phys. Lett. **99A**, 321 (1983); Moffat, J. Fluid Mech. **150**, 359 (1985); Farge, Pellegrino, & Schneider, PRL 87, 054501 (2001).

-1 red

+1 blue
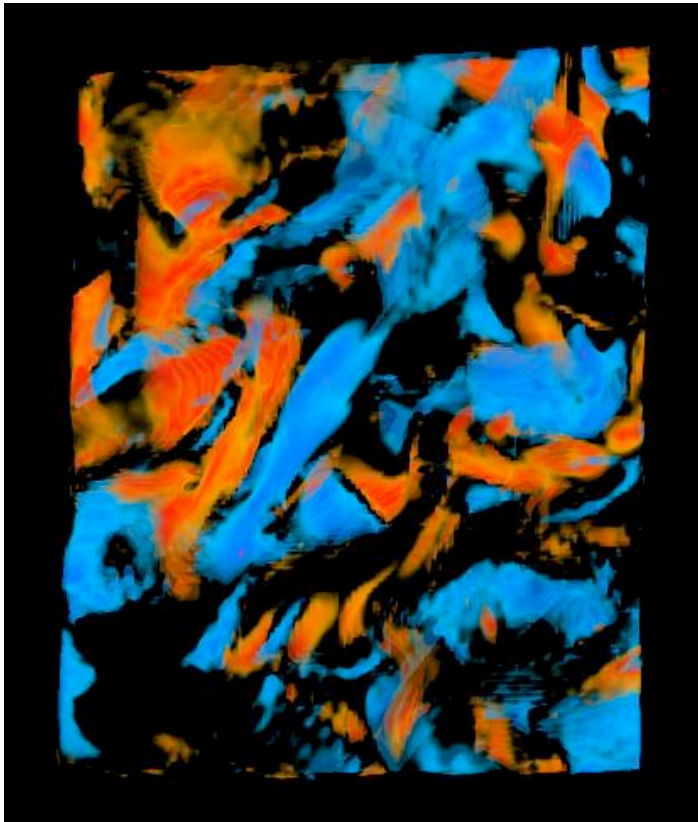
Large and small scale structures (TG)

- Another region showing local beltramization, for the same flow.
- Note that helicity has a large filling factor, even in the small scales.

-1 red

+1 blue
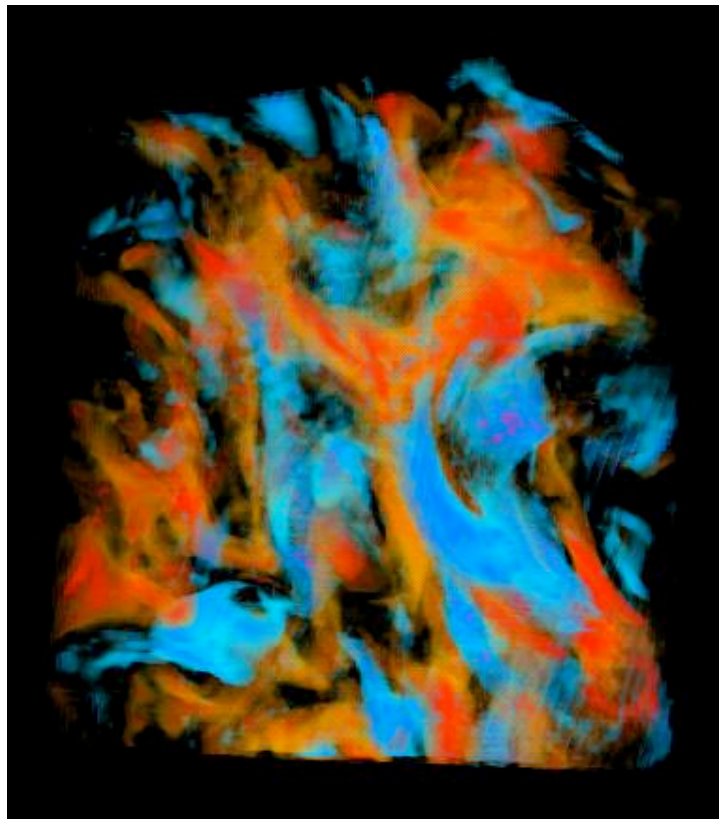
Energy spectrum and flux (TG)
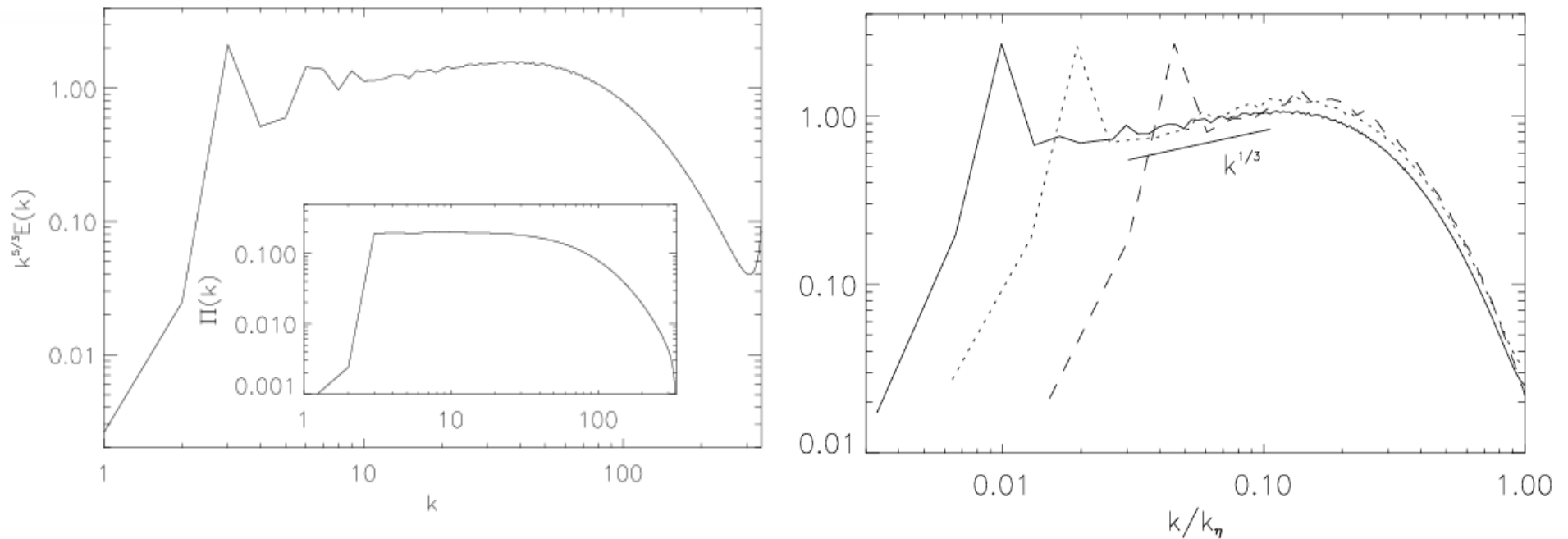
- Well developed (compensated) energy spectrum.
- Wide range of wave numbers with constant energy flux.
- Large resolution is needed to observe a Kolmogorov spectrum. At lower resolution mostly the bottleneck is observed.
- The bottleneck seems to follow a $k^{-4/3}$ power law. Kurien, Taylor, & Matsumoto **69**, 066313 (2004).

Energy and helicity spectra (ABC)
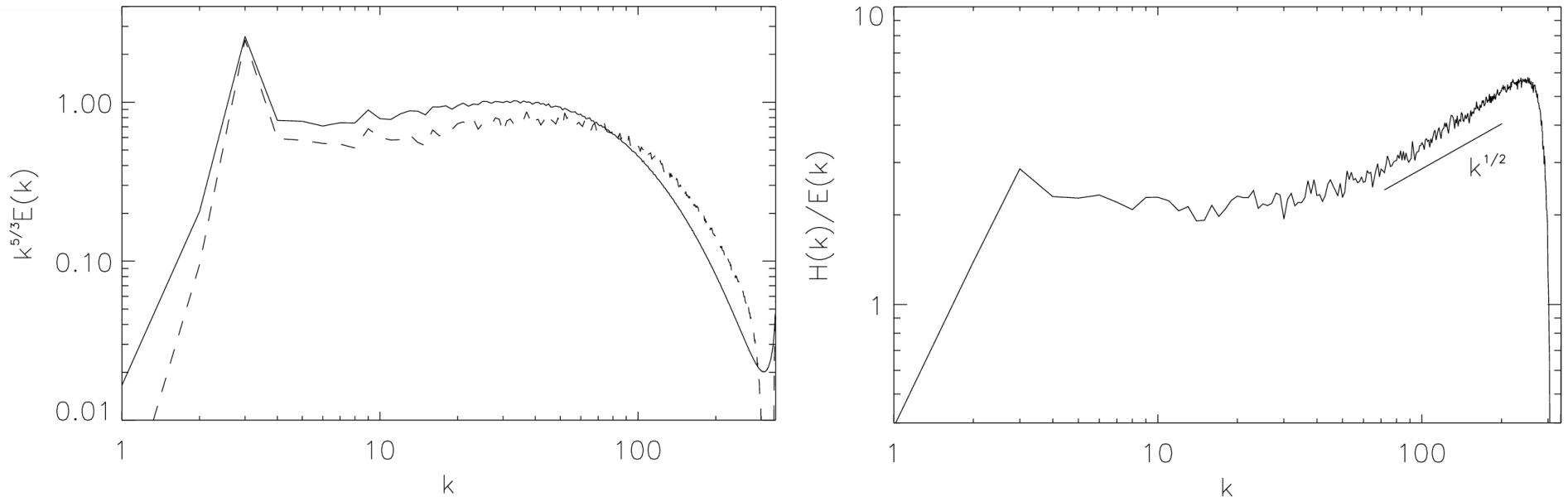
- Well developed (compensated) energy and helicity spectra.
- The helicity follows a Kolmogorov power law. Chen, Chen, Eyink, & Holm, PRL **90**, 214503 (2003); Gomez & Mininni, Physica A **342**, 69 (2004).
- As a result, the relative helicity $H(k)/(kE(k))$ should drop as k^{-1}. But helicity persists at small scales and a pile up of relative helicity is observed in the dissipative range.

Transverse velocity increments
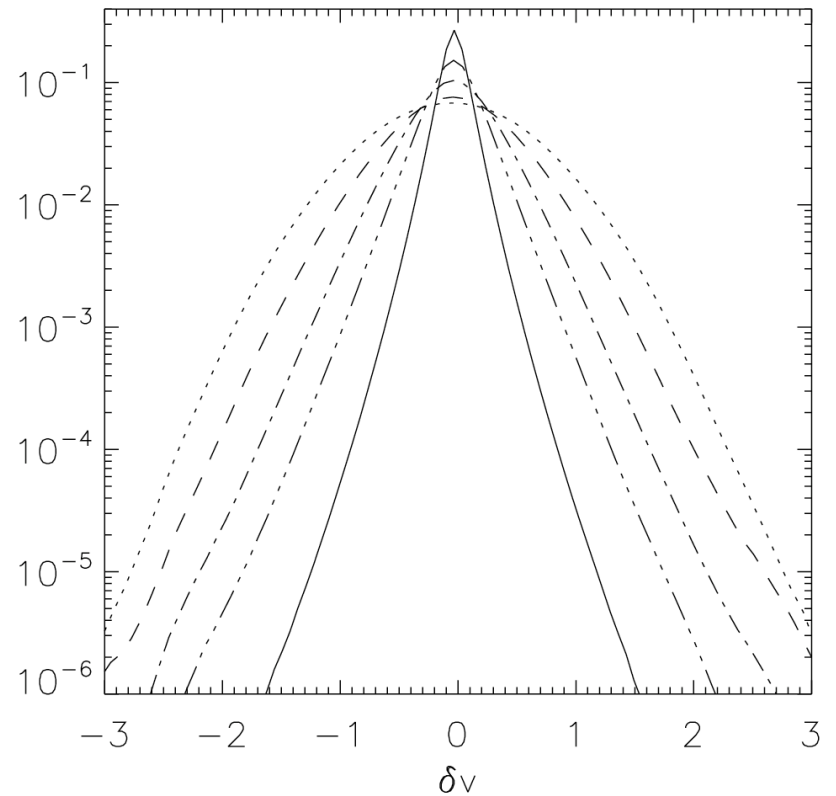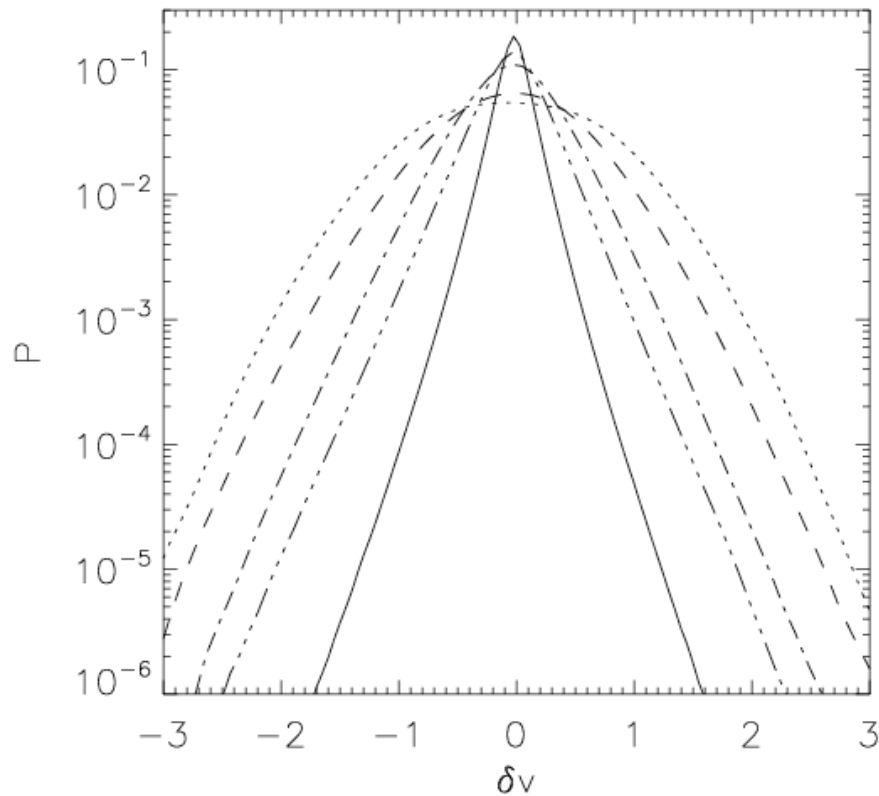
- PDFs of velocity increments $\delta v = \langle \mathbf{v}_\perp(\mathbf{x}+\mathbf{l}) - \mathbf{v}_\perp(\mathbf{x})] \rangle$
- TG (right) and ABC (left).

Intermittency: time series
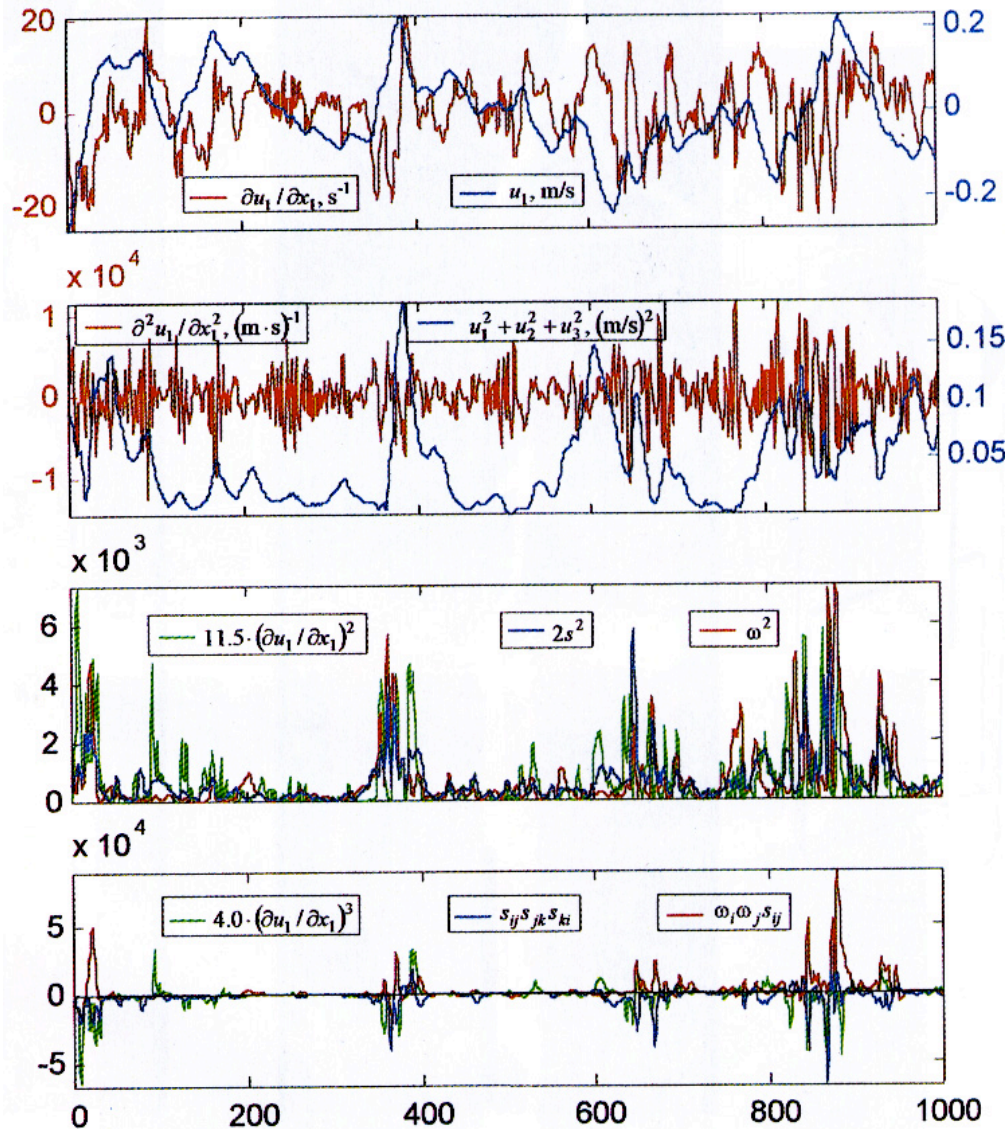
- Observations in the PBL Kholmyansky and Tsinober (2000)

- Note the intermittent nature of the signals associated with velocity derivatives.

- Peaks with are hundreds times larger than the mean are not rare.

Velocity increments and intermittency

- The non-gaussian tails in the PDFs of velocity increments are often associated to intermittency.

- The closer the two points (the smaller the scale), the more the PDFs deviate from a Gaussian distribution, both in the center and in the tails.

- However, PDFs of velocity increments contain no information of the structure of the underlying strong and weak events.

- Similar PDFs can have different underlying structures!

- What is the origin of intermittency?

  – Direct coupling between large and small scales

  – Singular structures

  – Multiplicative noise

Transverse velocity increments (TG)
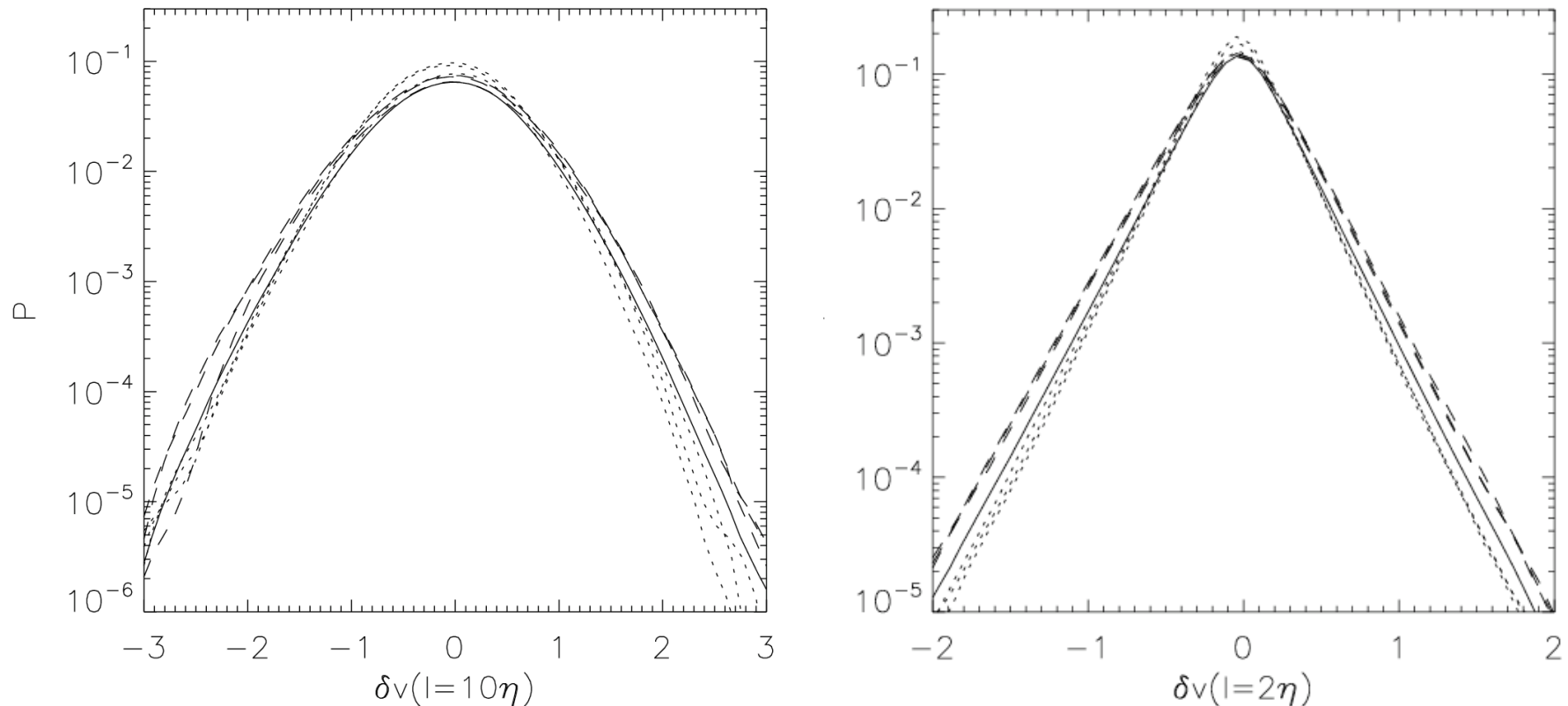
- In the TG flow, a correlation is observed between regions of large scale shear and regions with strong gradients in the small scales. Regions with strong large scale shear (dashed lines) have stronger tails.

Intermittency: structure functions

- For a component of a field f we define the longitudinal structure functions of order p as

$$\mathfrak{S}_p^f(l) \equiv \langle |\delta f|^p \rangle$$

where the longitudinal increment is given by

$$\delta \mathbf{f} = \mathbf{f}(\mathbf{x} + \mathbf{l}) - \mathbf{f}(\mathbf{x})$$

- If the flow is self-similar we expect a behavior

$$\mathfrak{S}_p^f(l) \sim l^{\zeta_p^f}.$$

K41 predicts $\zeta_p^v = p/3$

- In practice departures from K41 are observed, and the anomalous scaling observed in the data can be fitted by considering the local dissipation (averaged in small volumes) follows certain statistics.

Structure functions (TG)
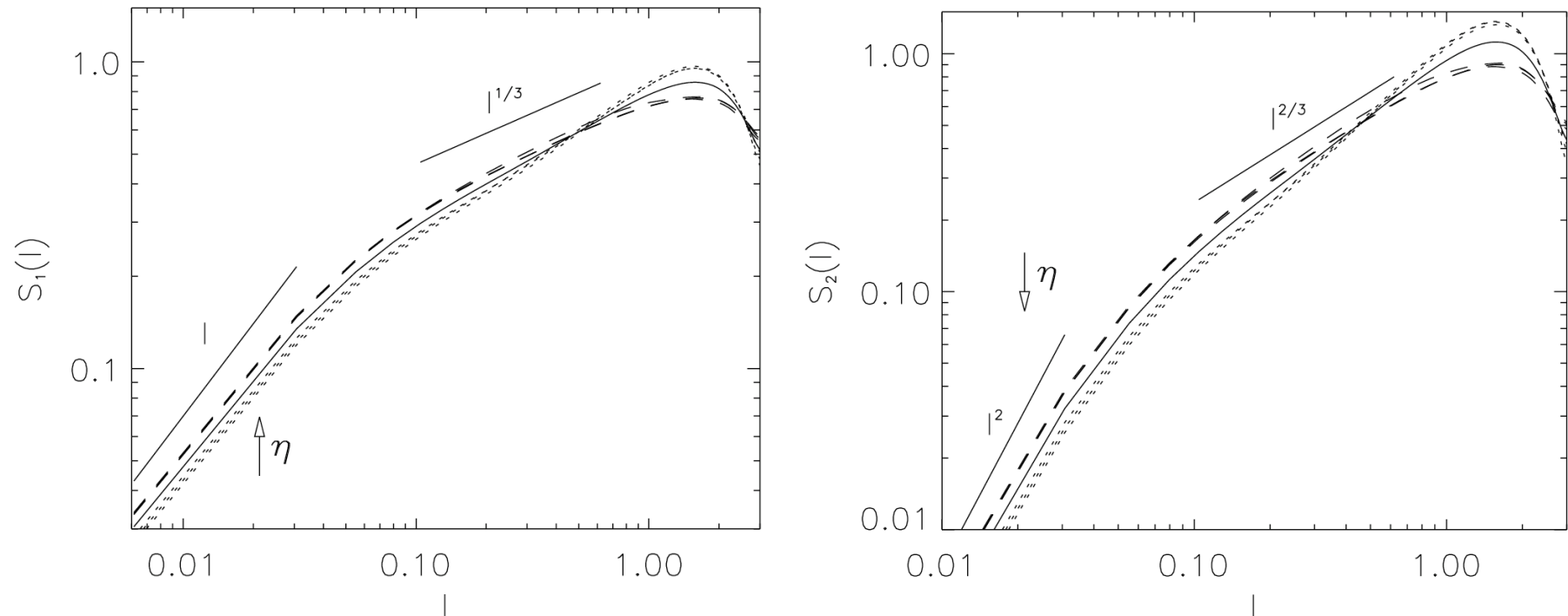
- Structure functions for longitudinal velocity increments $S_p(l) = \langle [v_{\parallel}(x+l) - v_{\parallel}(x)]^p \rangle$. In K41, $S_p(l) \sim l^{p/3}$. For a smooth flow, $S_p(l) \sim l^p$.

- A correlation is observed between regions of large scale shear and regions with strong gradients in the small scales.

Intermittency: structure exponents
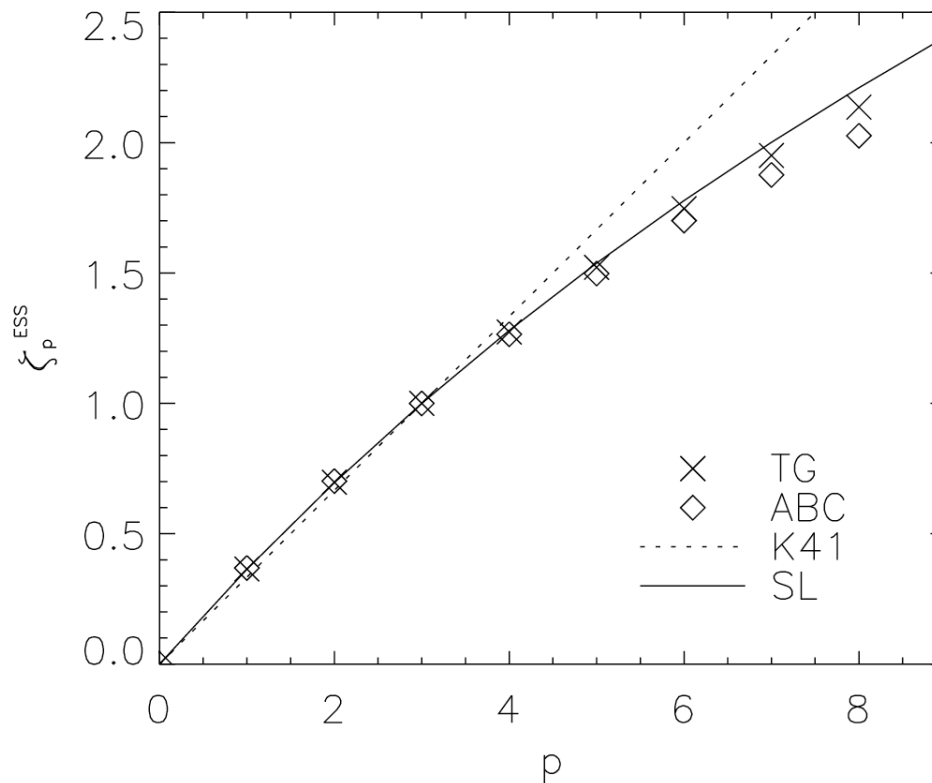
- Deviations from $S_p(l) \sim l^{p/3}$ are measured through the structure exponents: $S_p(l) \sim l^{\zeta_p}$.
- Small differences are observed in the ABC and TG simulations.
- What is the PDF of the energy dissipation?

Structure exponents and intermittency

- As in the PDFs, qualitatively different phenomena can possess the same set of scaling exponents.
- It is believed vortex tubes are associated to the intermittency. However, it is not clear what is the contribution of these structures to the exponents, or to the anomalous scaling.
- Are these quantities "universal"?
- The origin of intermittency in turbulent flows remains open.
- How to characterize intermittency is also an open problem.
- The existence of scaling exponents is a problem: if the Euler (or Navier-Stokes) equations have scaling symmetries, should statistical quantities have such symmetries too?

Why are structure functions important?
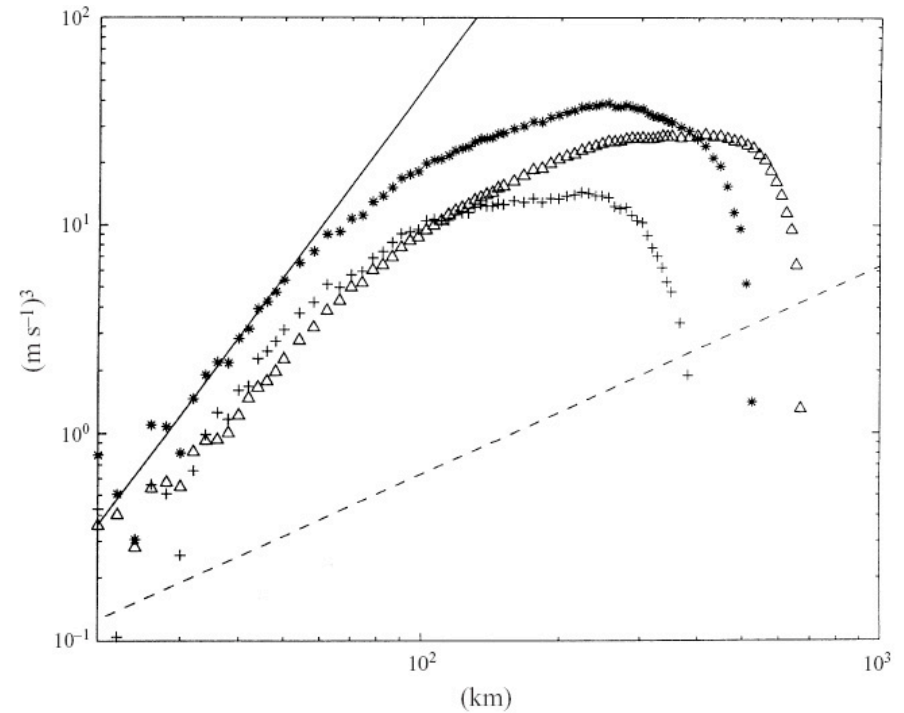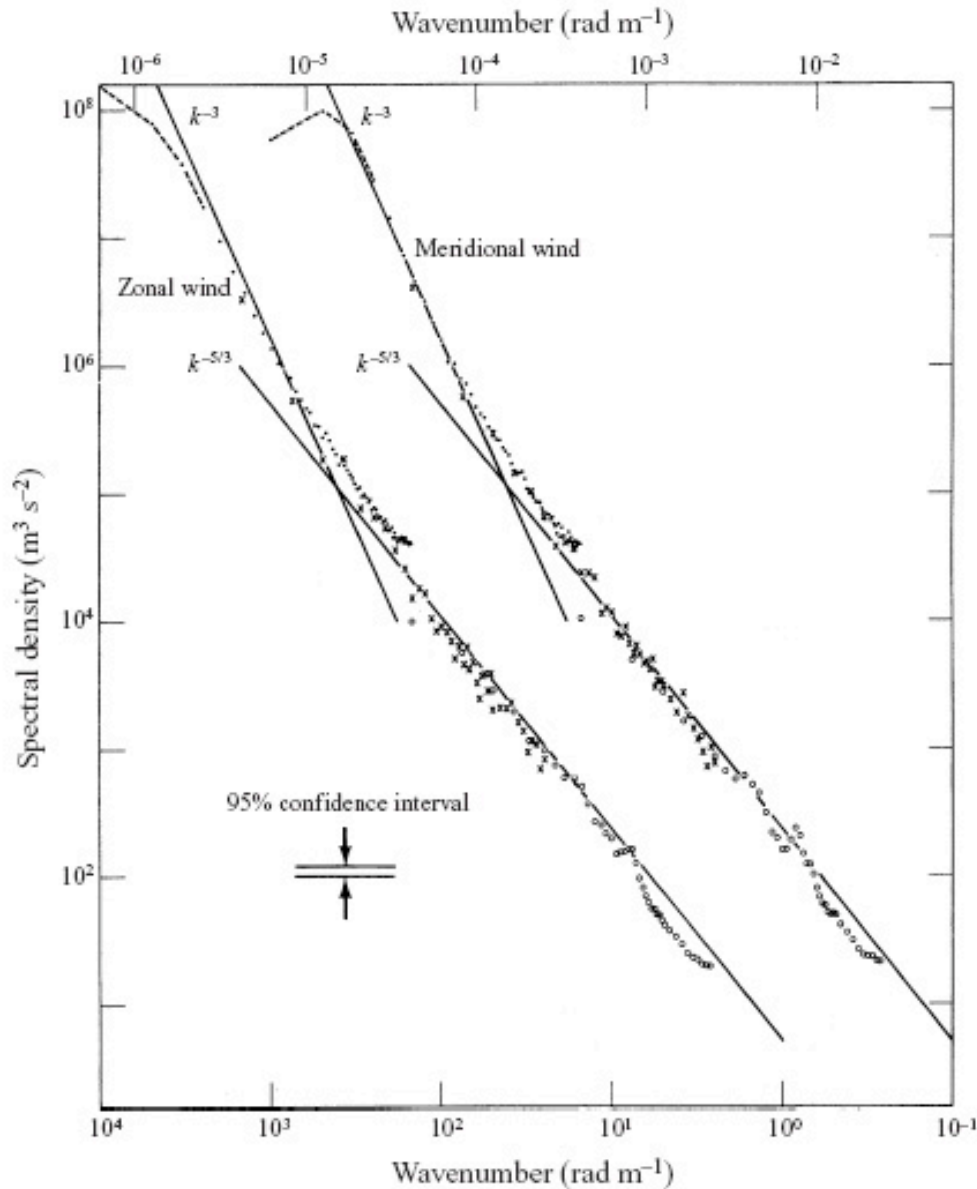
- Since $S_3(l) \sim \varepsilon\, l^{\,p/3}$, the sign of S_3 can be used to discriminate between a inverse and direct cascades of energy Lindborg (1999)

Why are structure functions important?
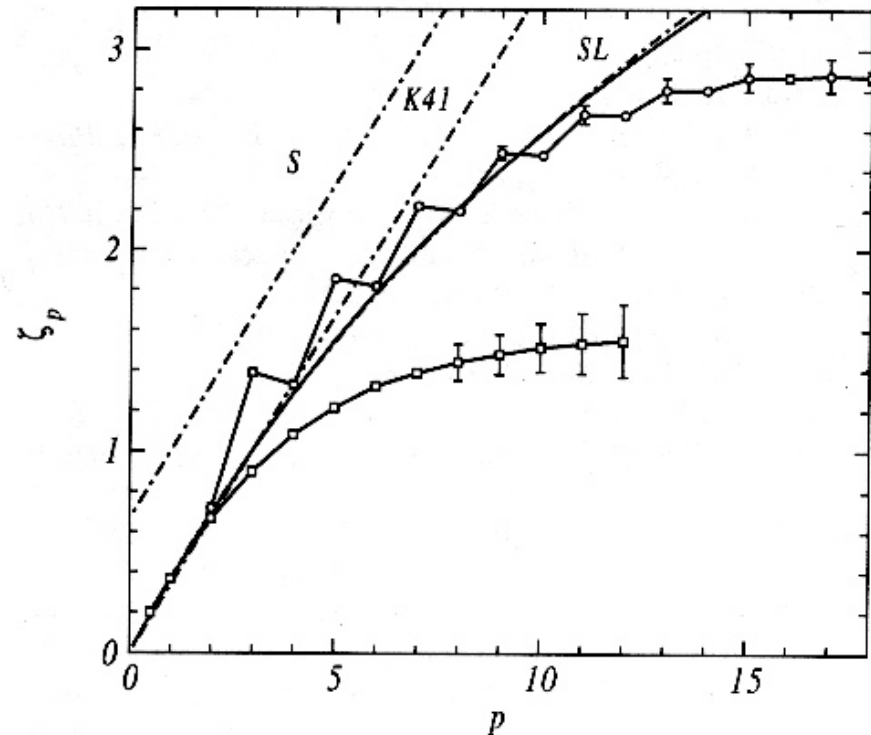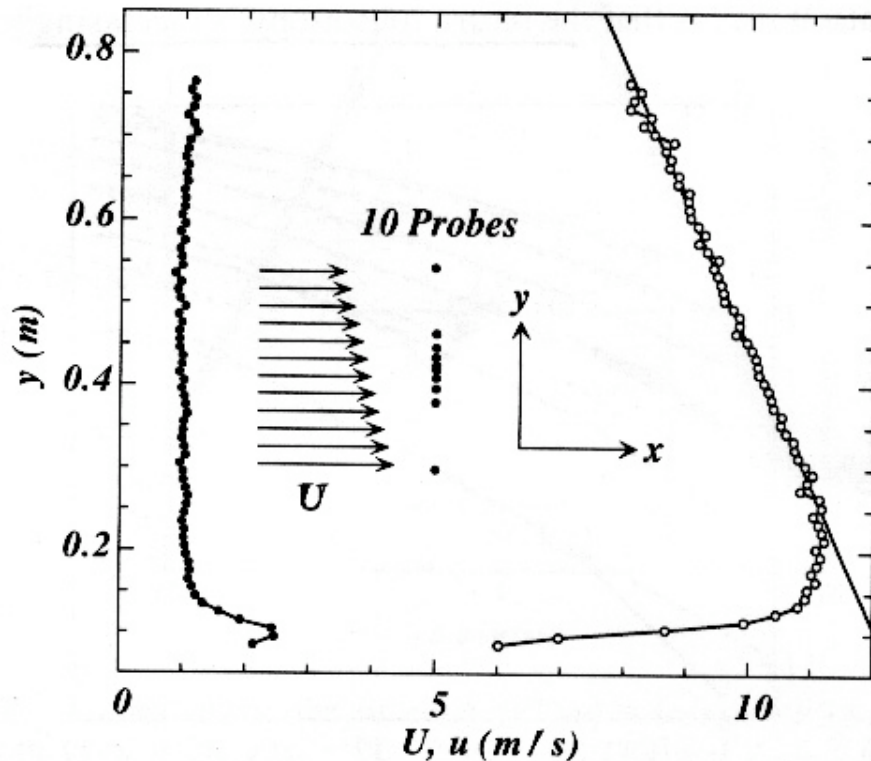
- If isotropy is recovered in the small scales (local interactions between scales), then odd moments of the velocity increments should be zero.

- However, a persistence of the anisotropy is observed in the small scales
  Staicu and van de Water (2003)

Energy transfer and triadic interactions

- The evolution of the kinetic energy in shells in Fourier space is

$$\frac{dE(k)}{dt} = -\sum_{p,q}\int \mathbf{v}_k \cdot \left[\left(\mathbf{v}_p \cdot \nabla\right)\mathbf{v}_q\right]d^3x - 2\nu\Omega(k) + F(k)$$

- We can define

$$T(k,p,q) = -\int \mathbf{v}_k(\mathbf{x})\cdot\left[\mathbf{v}_p(\mathbf{x})\cdot\nabla\mathbf{v}_q(\mathbf{x})\right]d^3x$$

$$T(k,q) = -\int \mathbf{v}_k(\mathbf{x})\cdot\left[\mathbf{v}(\mathbf{x})\cdot\nabla\mathbf{v}_q(\mathbf{x})\right]d^3x$$

$$T(k) = -\int_k \mathbf{v}_k(\mathbf{x})\cdot\left[\mathbf{v}(\mathbf{x})\cdot\nabla\mathbf{v}(\mathbf{x})\right]d^3x$$

$$\Pi(k) = -\int_0 T(k)dk$$

The transfer satisfies the relation $T(k,q) = -T(q,k)$.

$\mathbf{k} = \mathbf{p} + \mathbf{q}$

Alexakis, Mininni, & Pouquet, PRE **95**, 264503
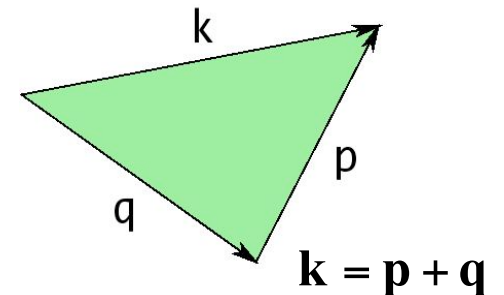
Energy transfer

- Transfer of energy from the shell q to the shell k, interacting with all modes with $p = |\mathbf{q}-\mathbf{k}|$

$$T(k,q) = -\int \mathbf{v}_k(\mathbf{x}) \cdot \left[\mathbf{v}(\mathbf{x}) \cdot \nabla \mathbf{v}_q(\mathbf{x})\right] d^3 x$$

- Local transfer of energy through non-local triadic interactions, or local transfer of energy through local triadic interactions?
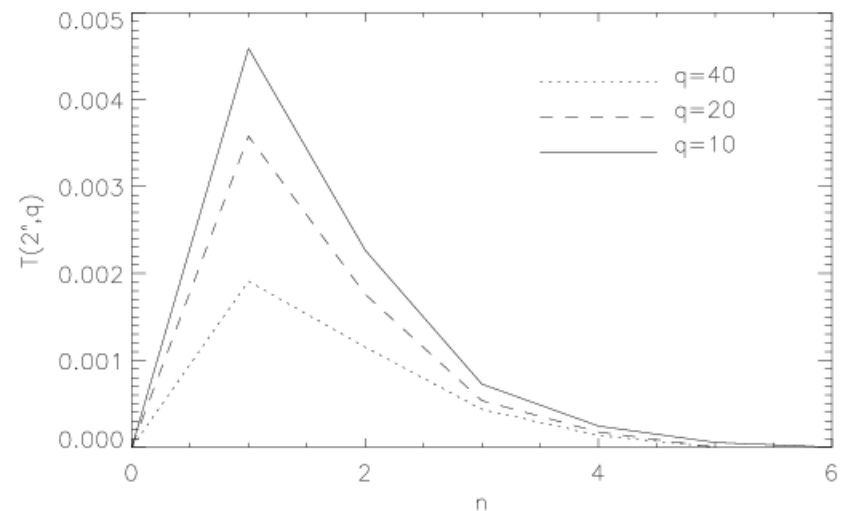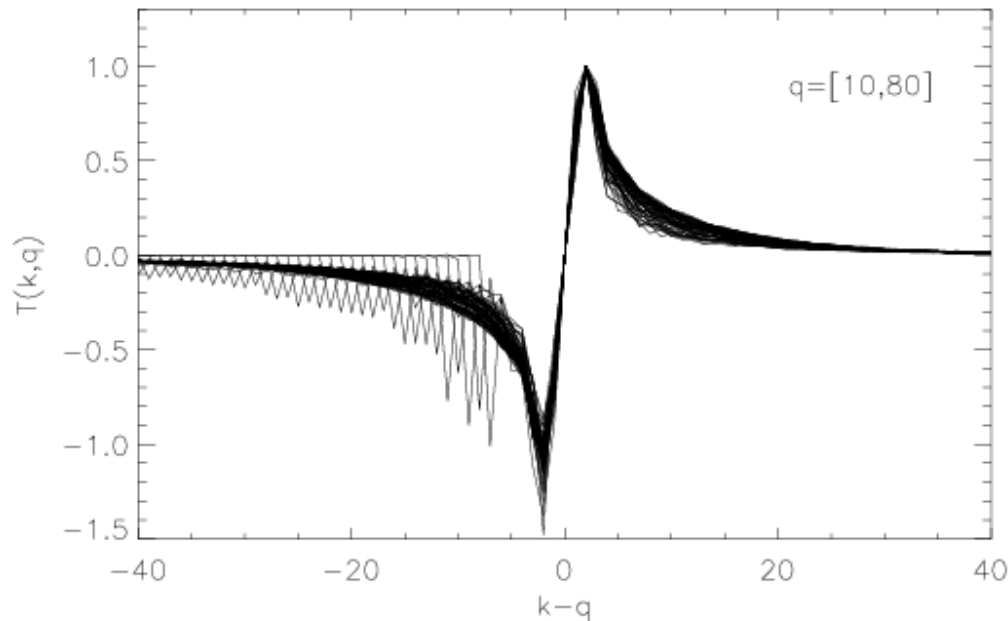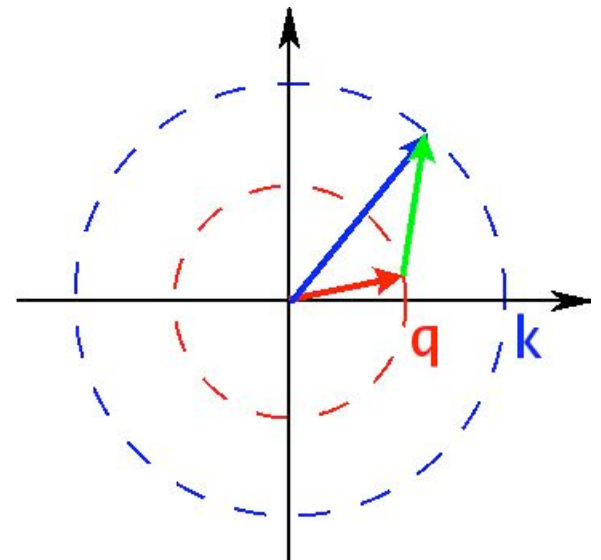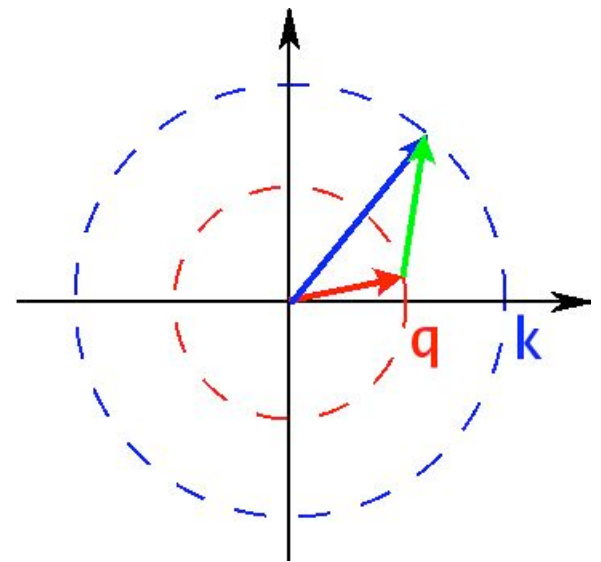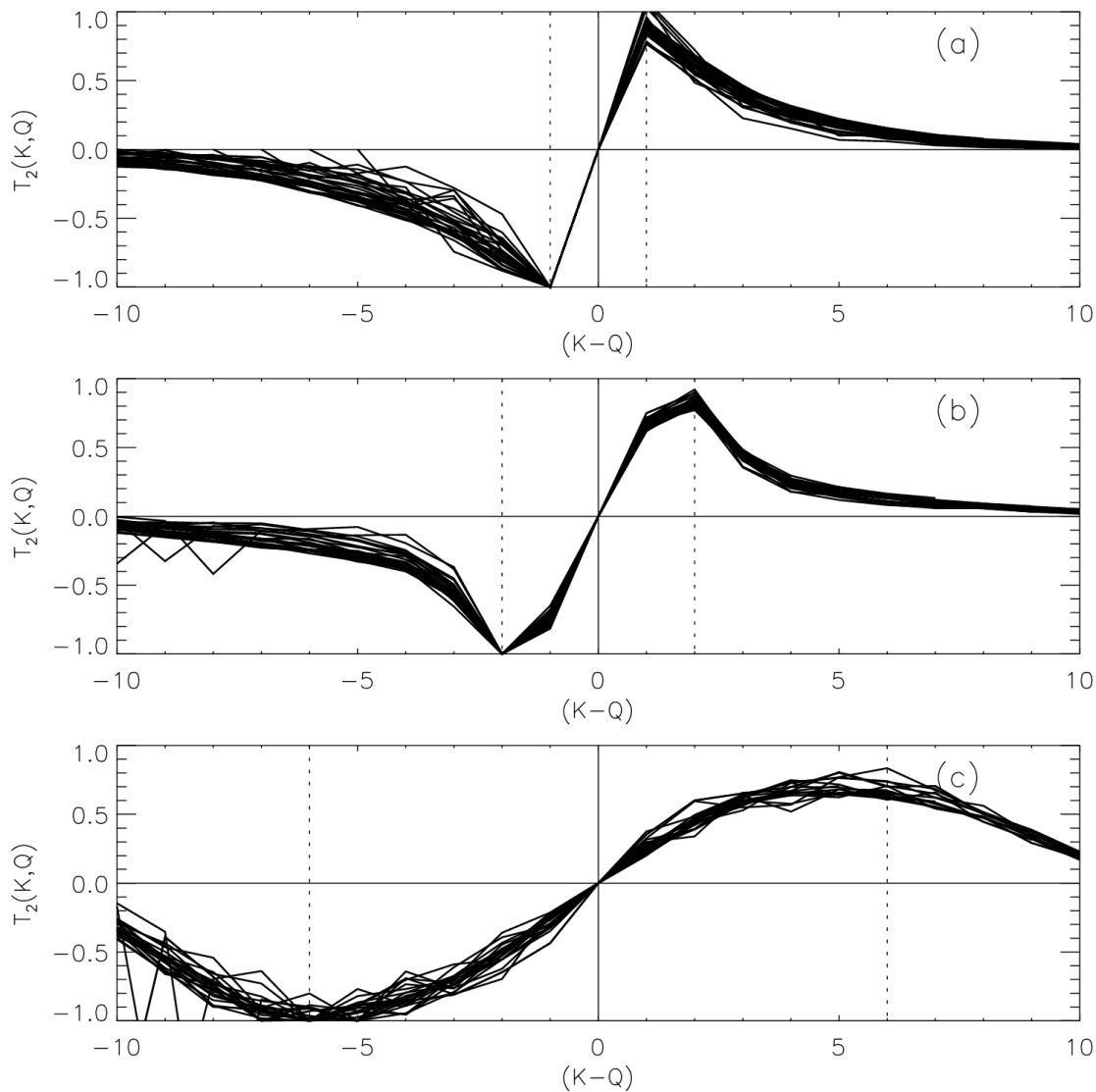
Triadic interactions

- If triadic interactions are local ($k \sim p \sim q$), the energy goes from the shell q to the shell $k \sim 2q$ (*i.e.* the transfer takes place in octave bands $k = 2^n$).

$$\mathbf{k} = \mathbf{p} + \mathbf{q}$$
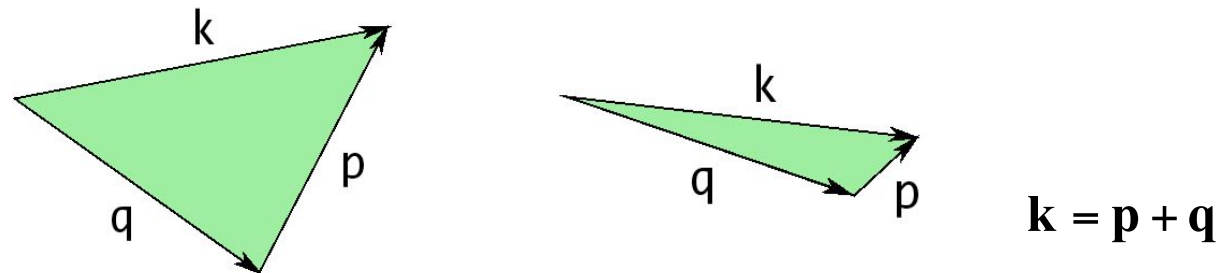
- The transfer $T(k,q)$ in our simulation peaks at $k \sim q+k_0$ for all values of q (elongated triangles).
- To identify the triadic interactions, we must study the transfer $T(k,p,q)$.
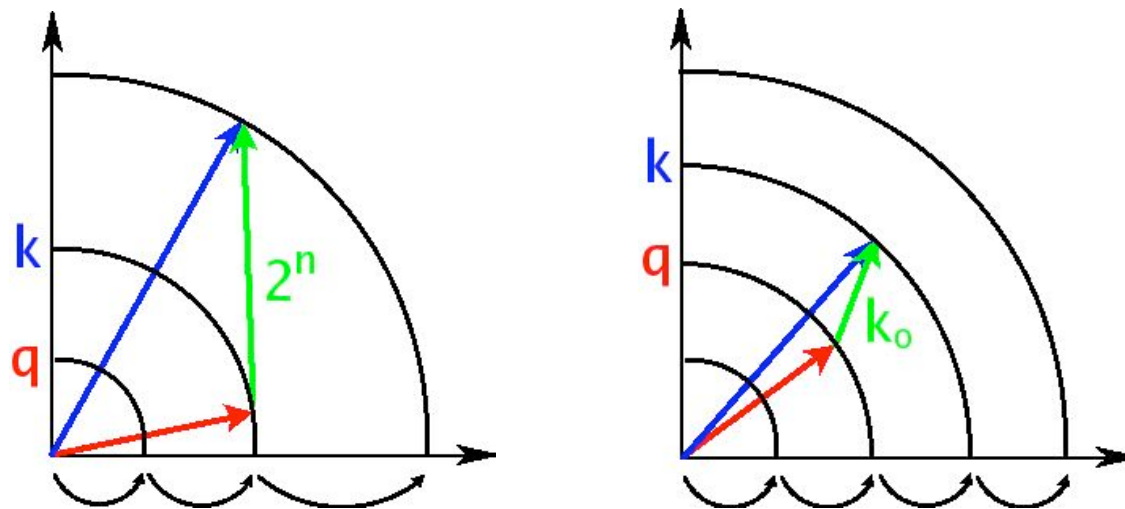
Energy transfer

- A set of simulations with random forcing at different wavenumbers confirms the dependence of the peak with the forcing wavenumber.

Energy transfer and triadic interactions

- We computed the transfer

$$T(k,p,q) = -\int \mathbf{v}_k(\mathbf{x}) \cdot \left[\mathbf{v}_p(\mathbf{x}) \cdot \nabla \mathbf{v}_q(\mathbf{x}) \right] d^3x$$

  for three values of *q* (10, 20, and 40).

- Transfer of energy from *q=10* to the shell *k*, interacting with modes in the shell *p*.

- The strongest interactions are for *p = 3*.

- Integrating *T(k,p,q)* over *p* up to *q/2* we obtain the contribution due to non-local triads.
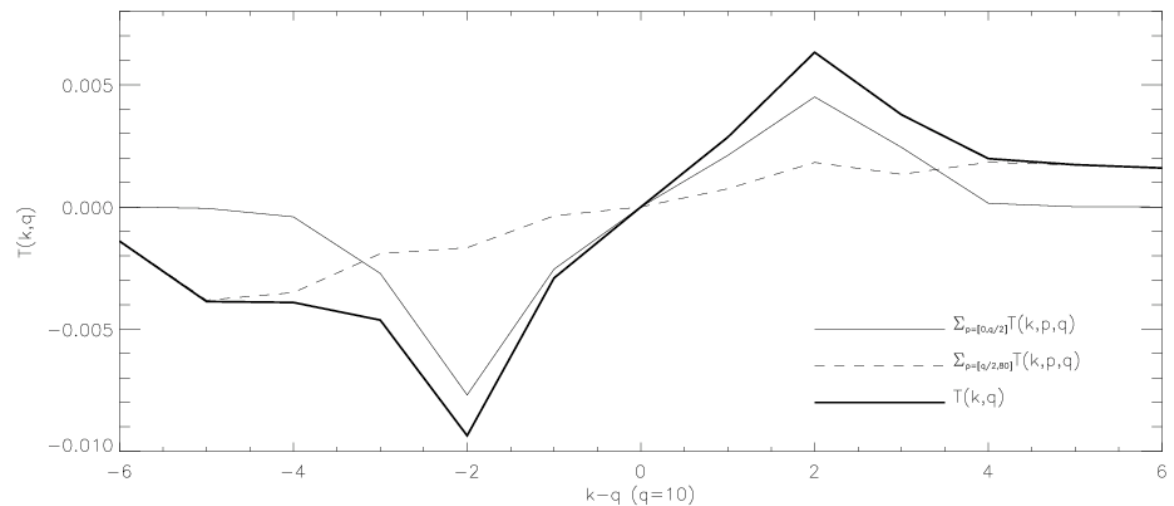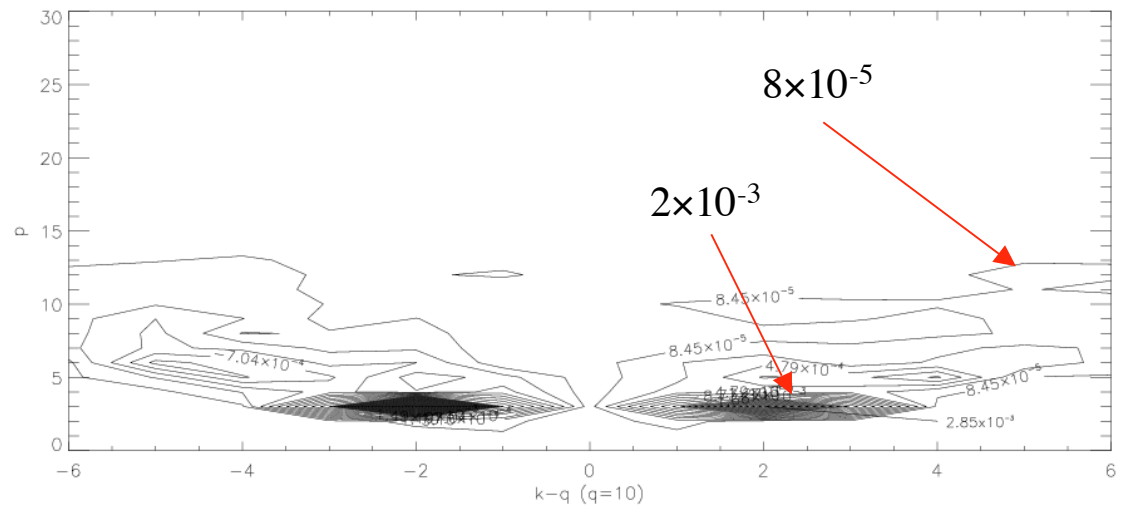
Energy transfer and triadic interactions

- Transfer of energy from the shell *q=20* to the shell *k*, interacting with modes in the shell *p*.
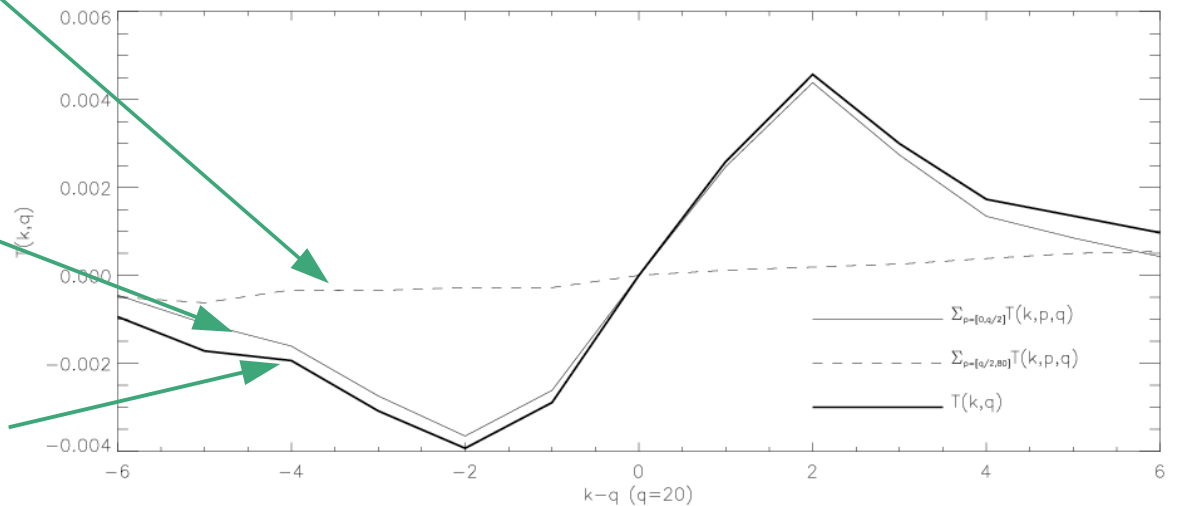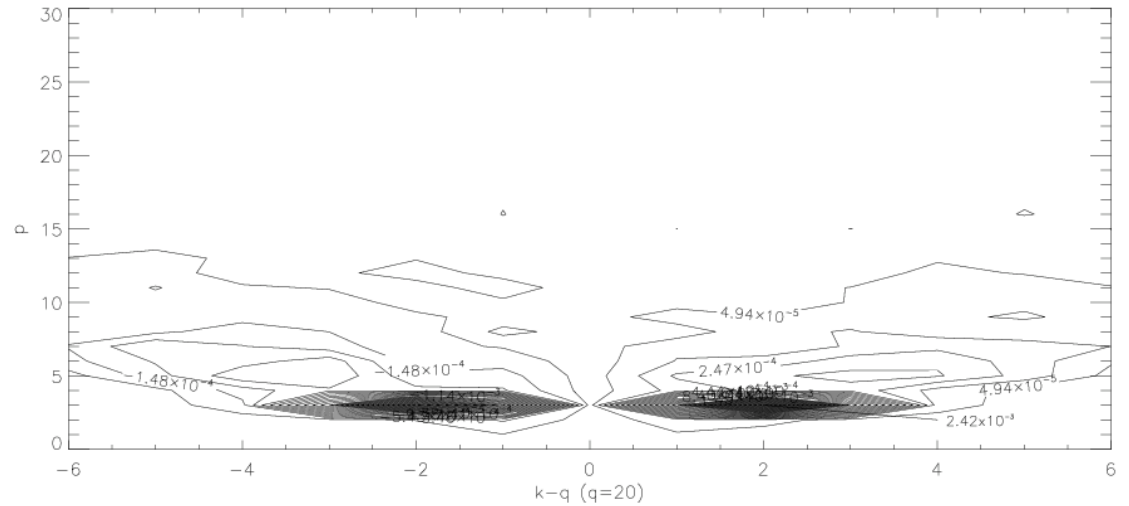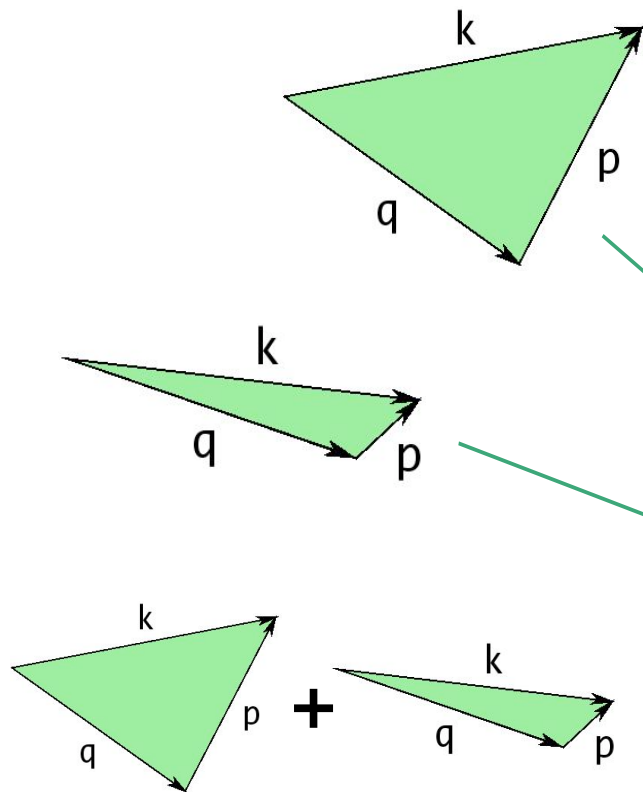
Energy transfer and triadic interactions

- Contour levels of $T(k,p,q)$, from the shell $q=40$ to the shell k, interacting with modes in the shell p.

- Local triadic interactions are weaker than interactions with the large scale flow.

- Local triads raise the tails of $T(k,q)$, but the peak of the transfer is at $k \sim q+k_0$.
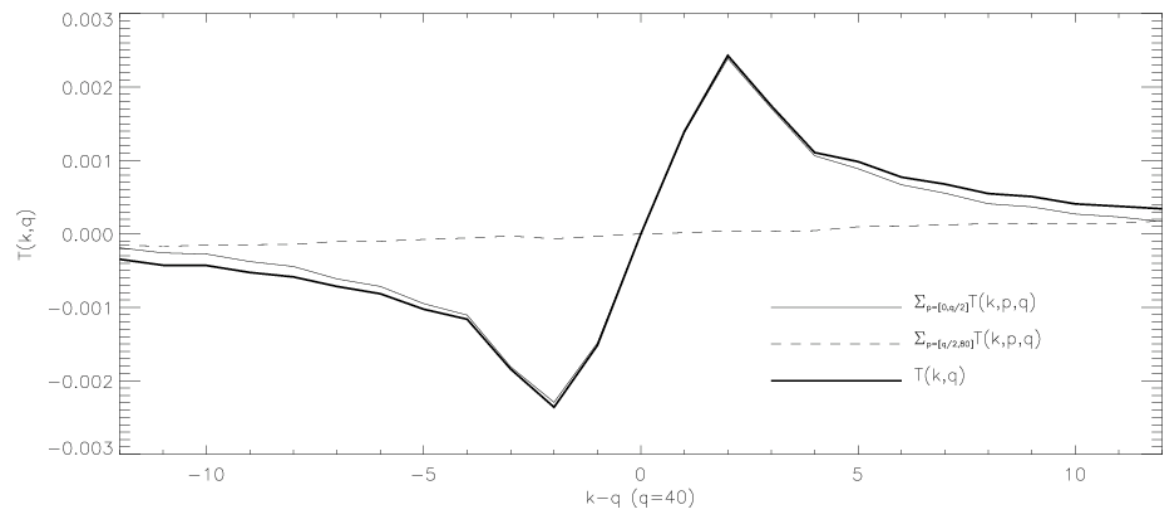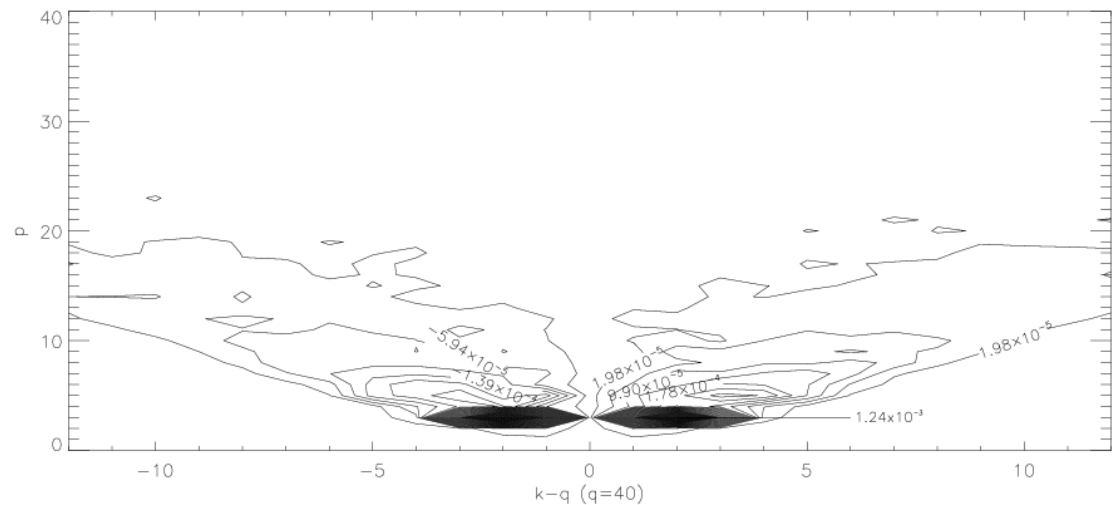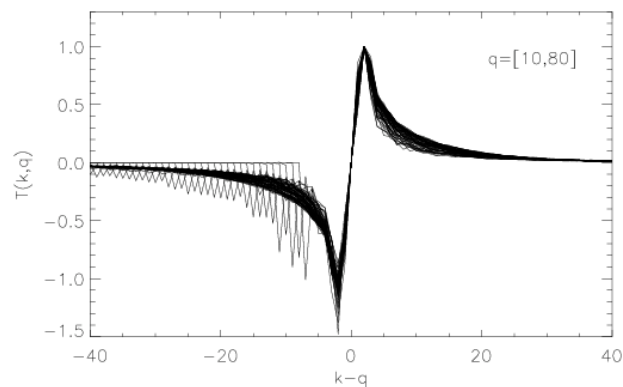
Energy transfer and flux

- Total flux

$$\Pi(k) = -\sum_{K=0}^{k} T_1(K)$$

$$= -\sum_{K=0}^{k} \sum_Q T_2(K, Q)$$

and flux from interactions with the large scale flow

$$P \approx k_0$$

and flux from nonlocal interactions

$$P < Q/2$$

- At the end of the inertial range, non local interactions are dominant.

- The ratio of the fluxes show that the large scale flow gives 20% of the total flux.

- Local triadic interactions are weaker, but give most of the energy flux.

- Is the bottleneck related to the dominance of non-local interactions in the dissipation range?
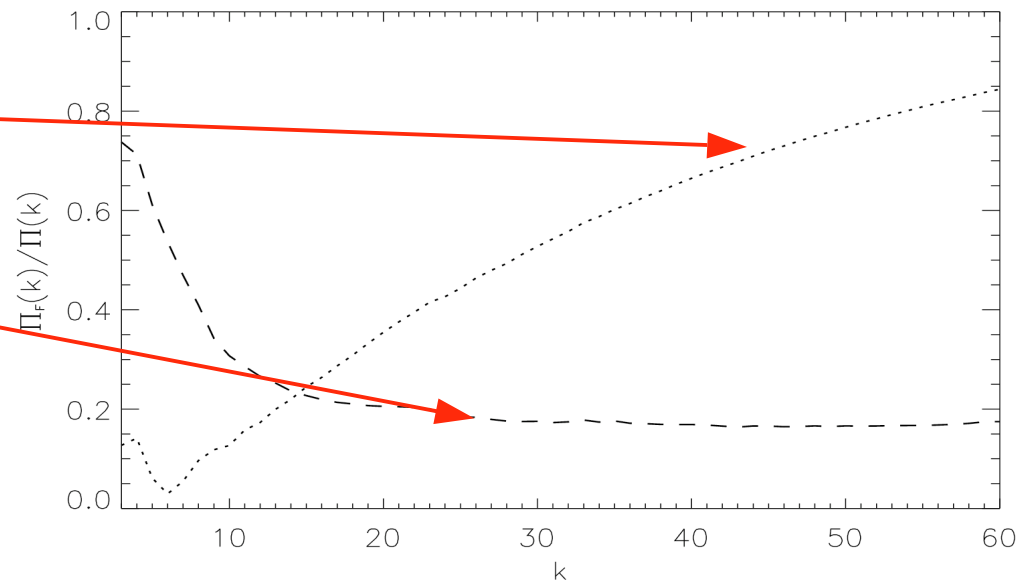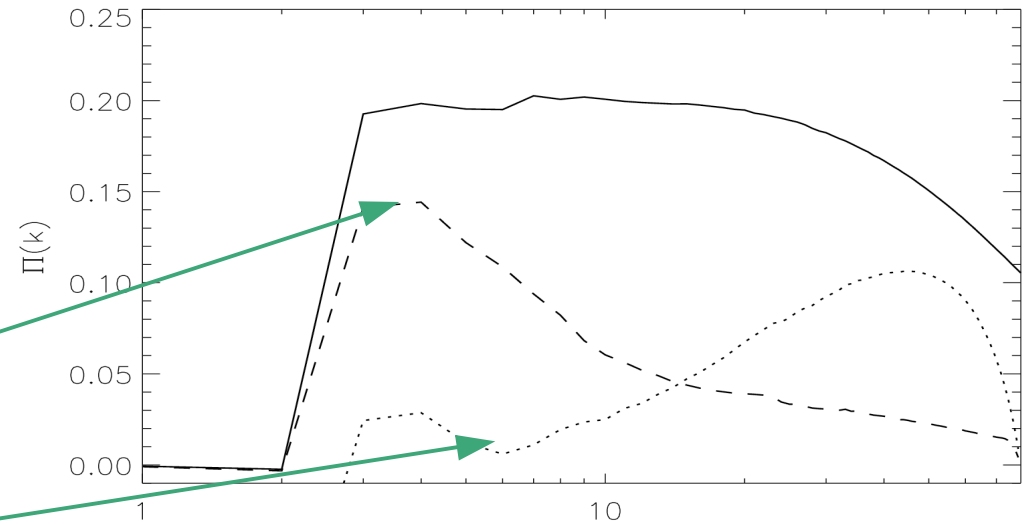
Evidence in experiments
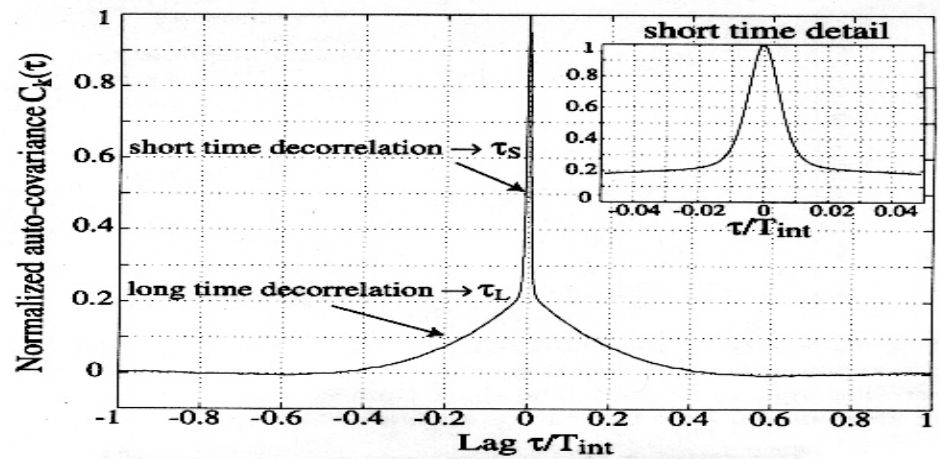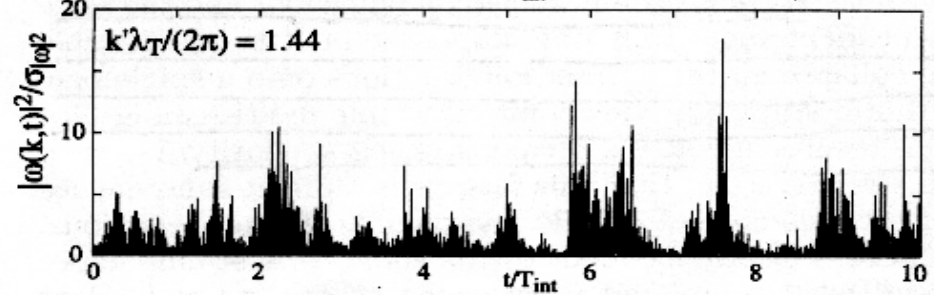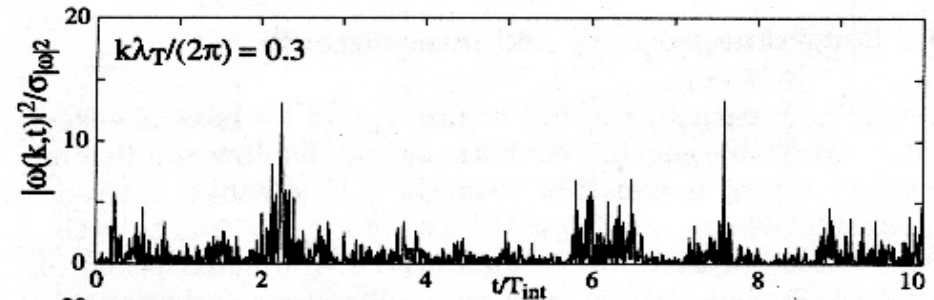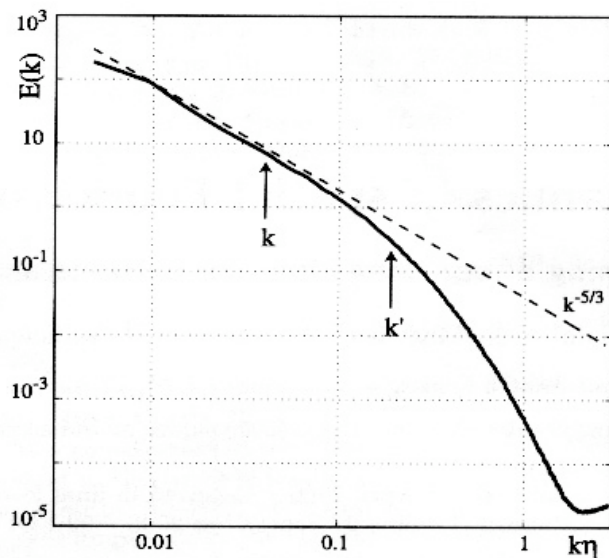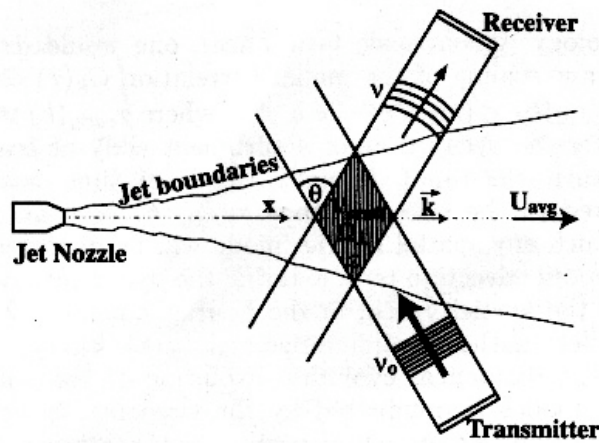
Poulain, Mazellier, Chevillard, Gagne, and Baudet (2006)

K41 and locality of interactions

- If shear is done by the large scale flow, distortion takes place at $1/\tau_L = U/L$.

- Then $\varepsilon \sim u_l^2 U/L$, and the energy spectrum is $E(k) \sim k^{-1}$! (as in RDT when only the large scale flow is considered).

- All these phenomenological arguments assume structures fill all space. But vortex filaments are not space filling.

- Non-local interactions with the large scale flow have also been shown to be responsible for the intermittency. Laval et al., Phys. Fluids **13**, 1995 (2001)

- If we consider interactions with the large scale flow and relate the length with the volume of the vortex tubes, then $\varepsilon \sim u_l^2 U/(l^2 L)^{1/3}$.

- As a result, $u_l^2 \sim l^{2/3}$ and we recover $E(k) \sim k^{-5/3}$.
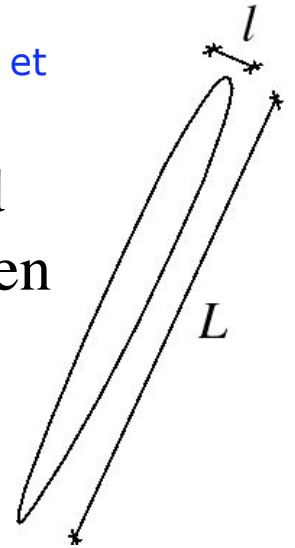
The MHD equations

- Momentum equation

$$\frac{\partial \mathbf{v}}{\partial t} + (\mathbf{v} \cdot \nabla)\mathbf{v} = -\nabla P + \mathbf{j} \times \mathbf{B} + \nu \nabla^2 \mathbf{v} + \mathbf{F}$$

- Induction equation

$$\frac{\partial \mathbf{B}}{\partial t} + \mathbf{v} \cdot \nabla \mathbf{B} = \mathbf{B} \cdot \nabla \mathbf{v} + \eta \nabla^2 \mathbf{B}$$

$$\mathbf{j} = \frac{c}{4\pi} \nabla \times \mathbf{B}$$

$$\mathbf{j} = \sigma (\mathbf{E} + \mathbf{v} \times \mathbf{B}/c)$$

$$\frac{1}{c}\frac{\partial \mathbf{B}}{\partial t} = -\nabla \times \mathbf{E}$$

- P is the pressure, $\mathbf{j}$ is the current, $\mathbf{F}$ an external force, ν the viscosity, η the resistivity, $\mathbf{v}$ the velocity, and $\mathbf{B}$ the induction (in Alfven velocity units); incompressibility is assumed.

The MHD equations

- Momentum equation:

$$\frac{\partial \mathbf{v}}{\partial t} + \left(\mathbf{v} \cdot \nabla \right) \mathbf{v} = -\nabla P + \mathbf{j} \times \mathbf{B} + \nu \nabla^2 \mathbf{v} + \mathbf{F}$$

$$\mathcal{T}_{uu}(Q, K) \equiv - \int \mathbf{u_K} (\mathbf{u} \cdot \nabla) \mathbf{u_Q} d\mathbf{x}^3 \quad \mathcal{T}_{bu}(Q, K) \equiv \int \mathbf{u_K} (\mathbf{b} \cdot \nabla) \mathbf{b_Q} d\mathbf{x}^3$$
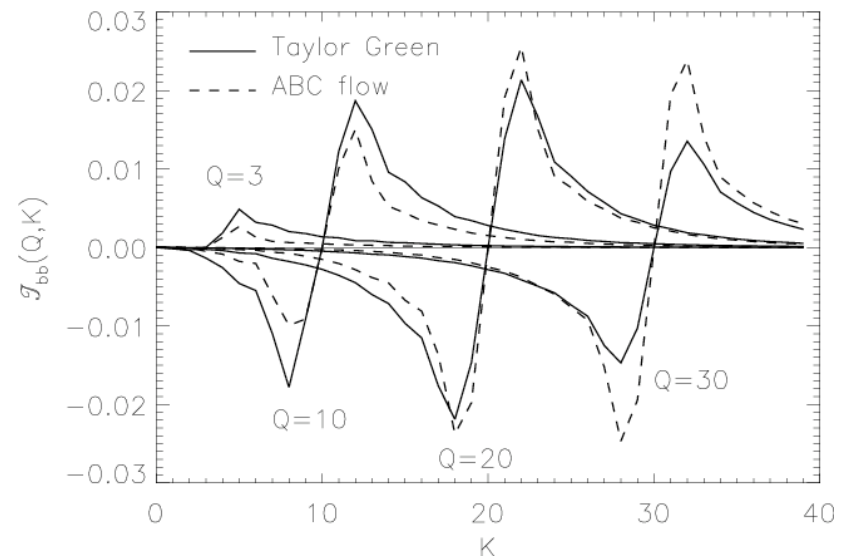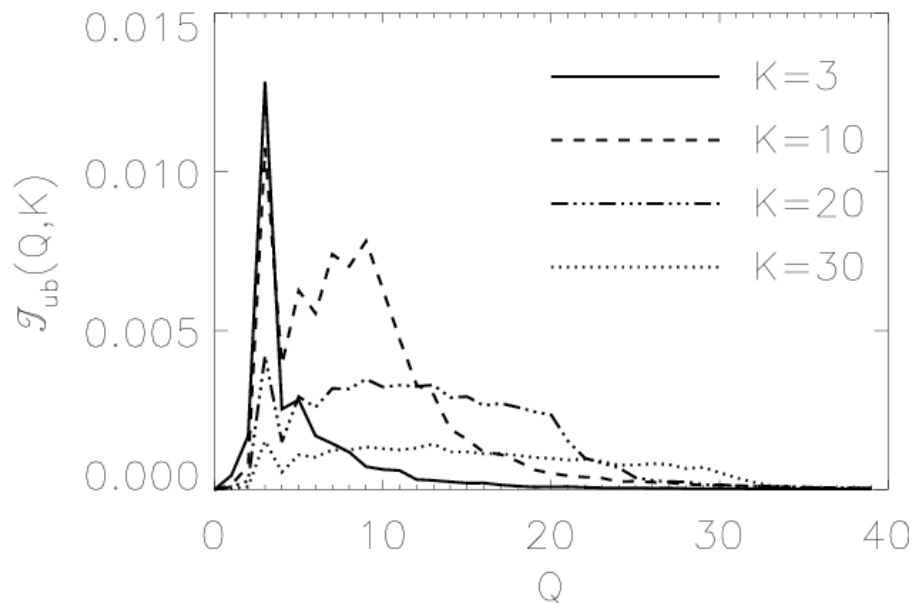
- Induction equation:

$$\frac{\partial \mathbf{B}}{\partial t} + \mathbf{v} \cdot \nabla \mathbf{B} = \mathbf{B} \cdot \nabla \mathbf{v} + \eta \nabla^2 \mathbf{B}$$

$$\mathcal{T}_{bb}(Q, K) \equiv - \int \mathbf{b_K} (\mathbf{u} \cdot \nabla) \mathbf{b_Q} d\mathbf{x}^3 \quad \mathcal{T}_{ub}(Q, K) \equiv \int \mathbf{b_K} (\mathbf{b} \cdot \nabla) \mathbf{u_Q} d\mathbf{x}^3$$
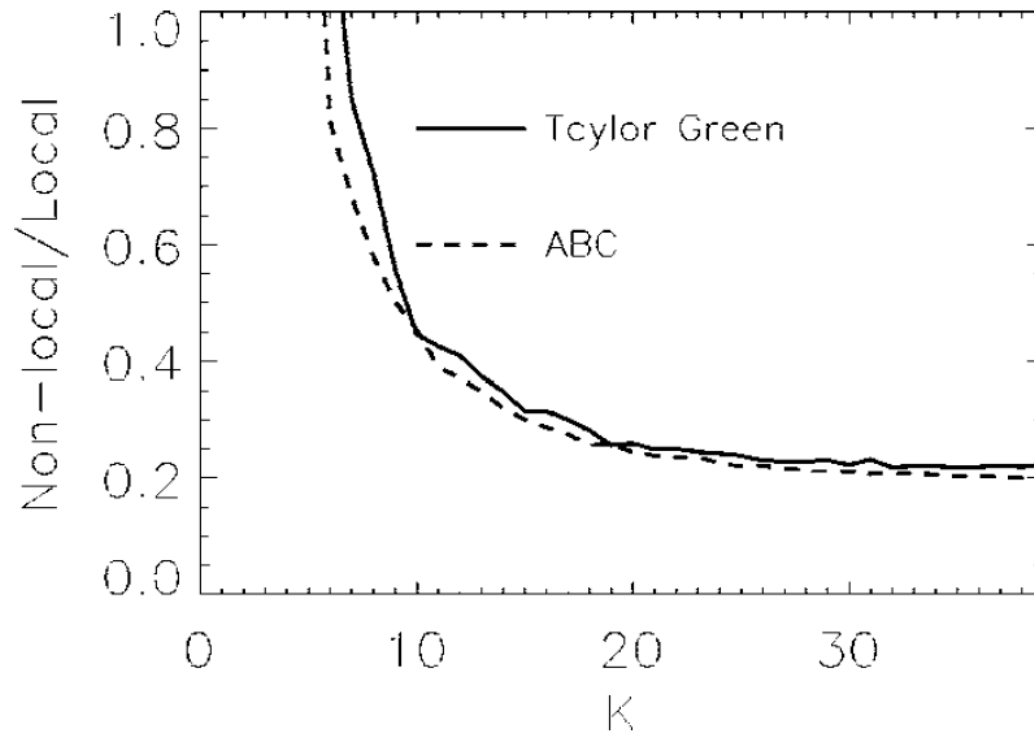
Alexakis, Mininni, & Pouquet, PRE 72, 046301 and 046302

The MHD transfer

- The **v→v** and **B→B** transfers *T(k,q)* are formally equivalent to the energy transfer in the hydrodynamic case and verified to be local in 256^3 MHD simulations.

- The **v→B** transfer (stretching of magnetic flux tubes) is nonlocal.

$$T_{\mathbf{vB}}(k,q) = -\int \mathbf{B}_k(\mathbf{x}) \cdot \left[\mathbf{B}(\mathbf{x}) \cdot \nabla \mathbf{v}_q(\mathbf{x})\right] d^3x$$

MHD turbulence: local vs. nonlocal

We can measure the ratio of energy received at a given wavenumber by nonlocal and local transfer:

$$\frac{NL}{L}(K) = \sum_{Q=1}^{K} \mathcal{T}_{ub}(Q,K) \bigg/ \sum_{Q=1}^{K} \mathcal{T}_{bb}(Q,K)$$

At small scales, 20% of the energy comes from non-local energy transfer.

MHD turbulence: structures

- 256^3 simulation.
- Regions with strong gradients (current sheets) are generated as the system evolves.
- Current sheets separate regions with magnetic field lines pointing in opposite directions.
- Later, the current sheets break down and a turbulent regime is reached.
- No vortex tubes can be recognized.
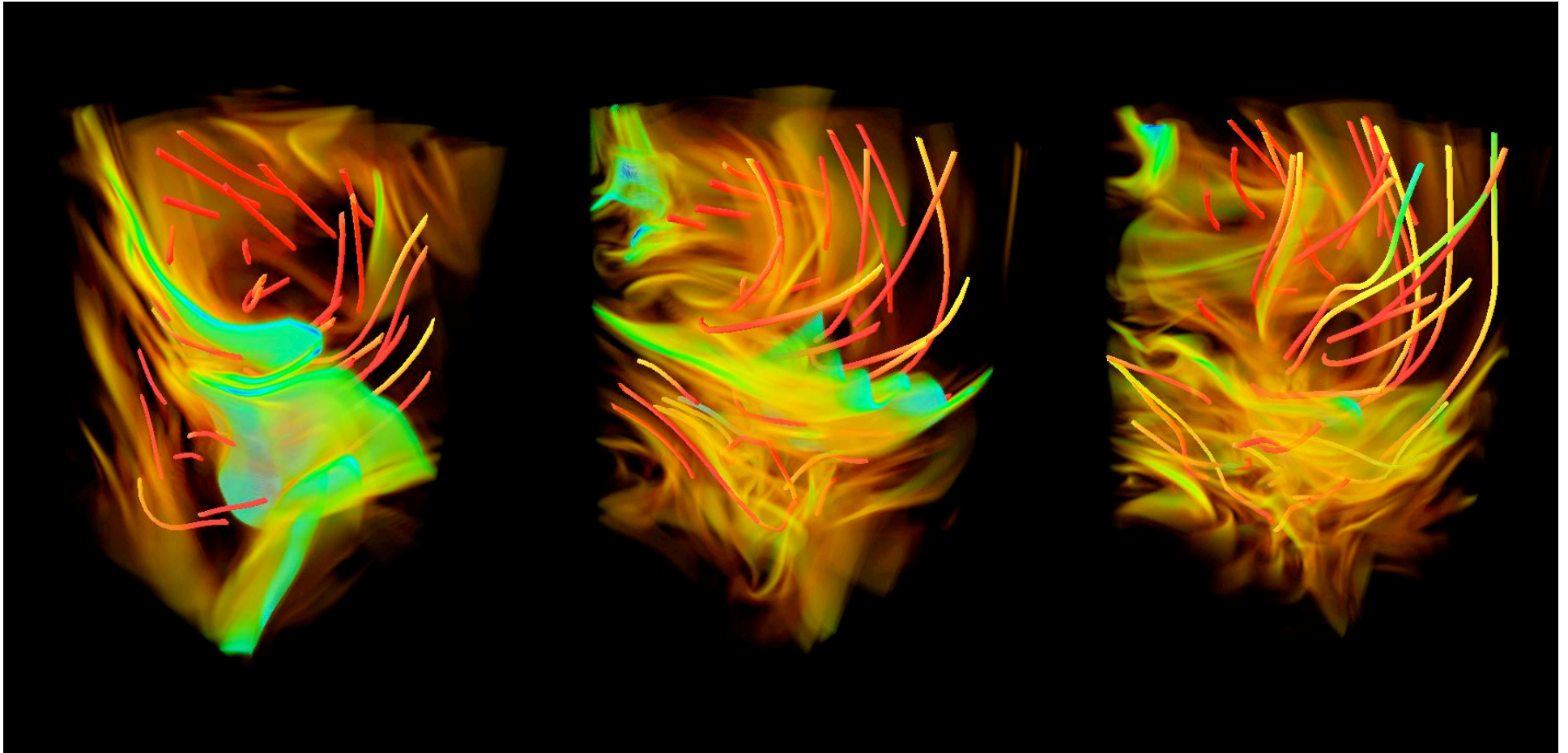- Is the fast generation of these structures associated with non-local effects in MHD?
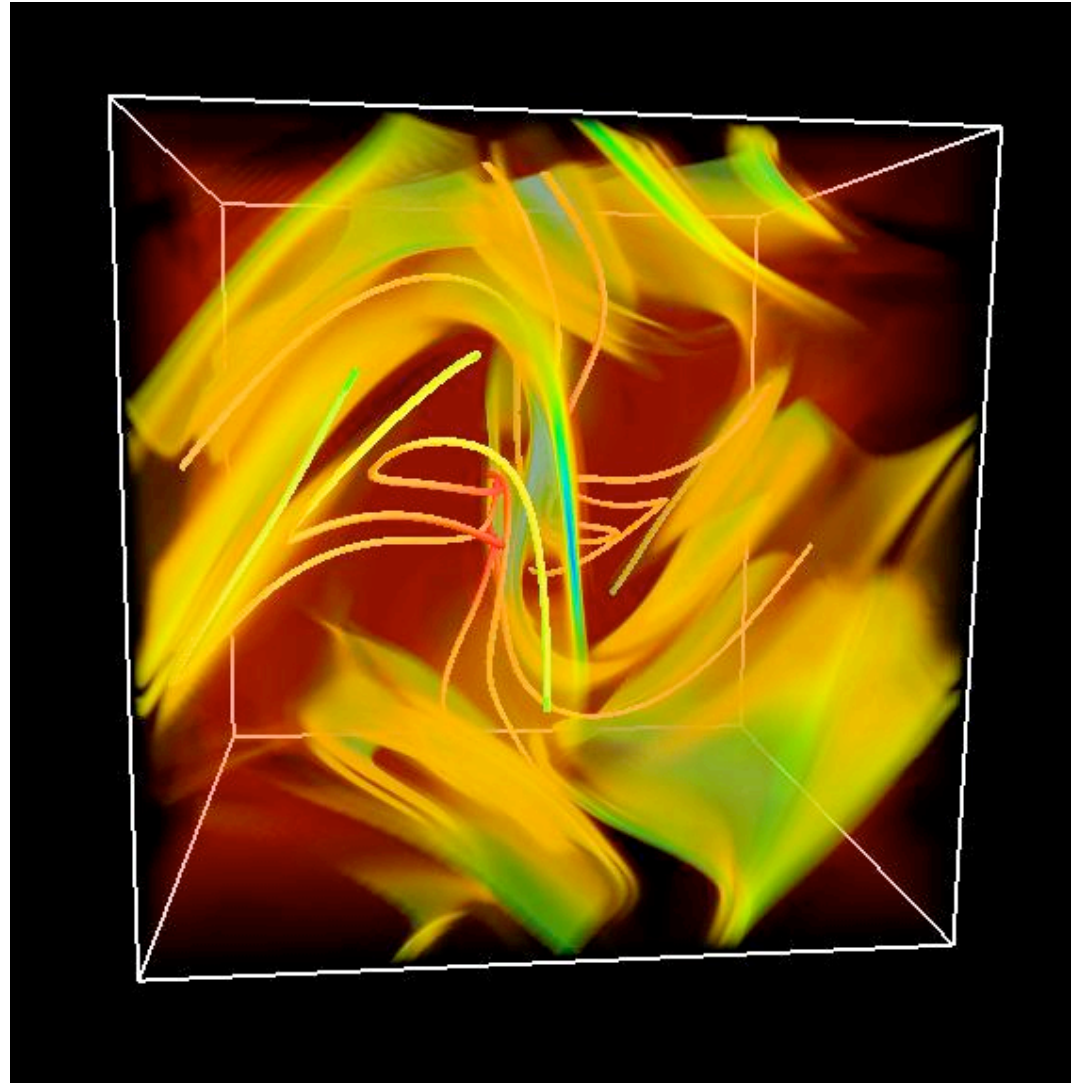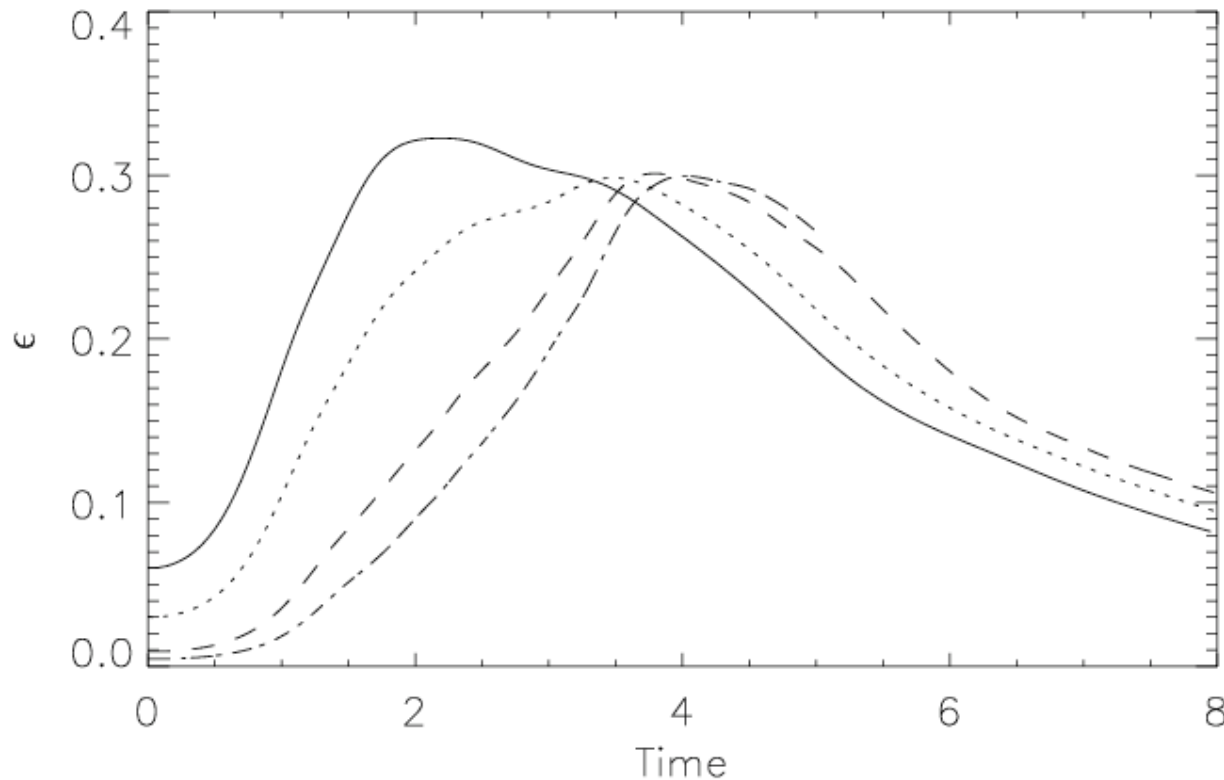
MHD turbulence: structures
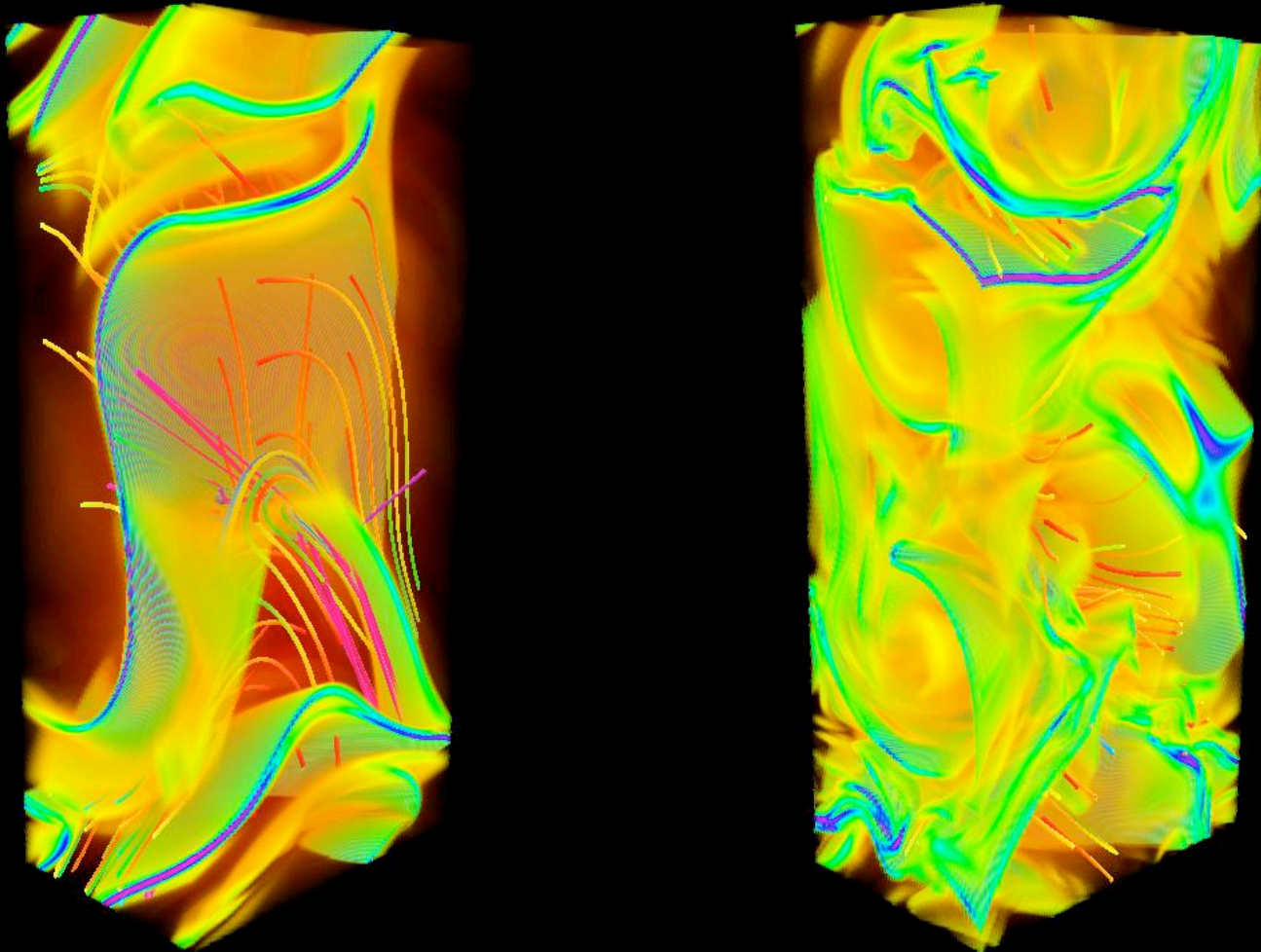
512³ Orszag-Tang

MHD turbulence: structures

- ABC flow in the large scales (helical) plus random initial conditions in the small scales.
- A small region in a 1536^3 simulation is shown.

Dissipation in MHD turbulence

- Is ε (the energy dissipation rate) constant in MHD turbulence at large Reynolds numbers?
- Kaneda's 4096^3 simulation gave convincing evidence in the hydrodynamic case.
- The figure shows ε(t) in several Orszag-Tang simulations at different *Re*.

Current sheet formation
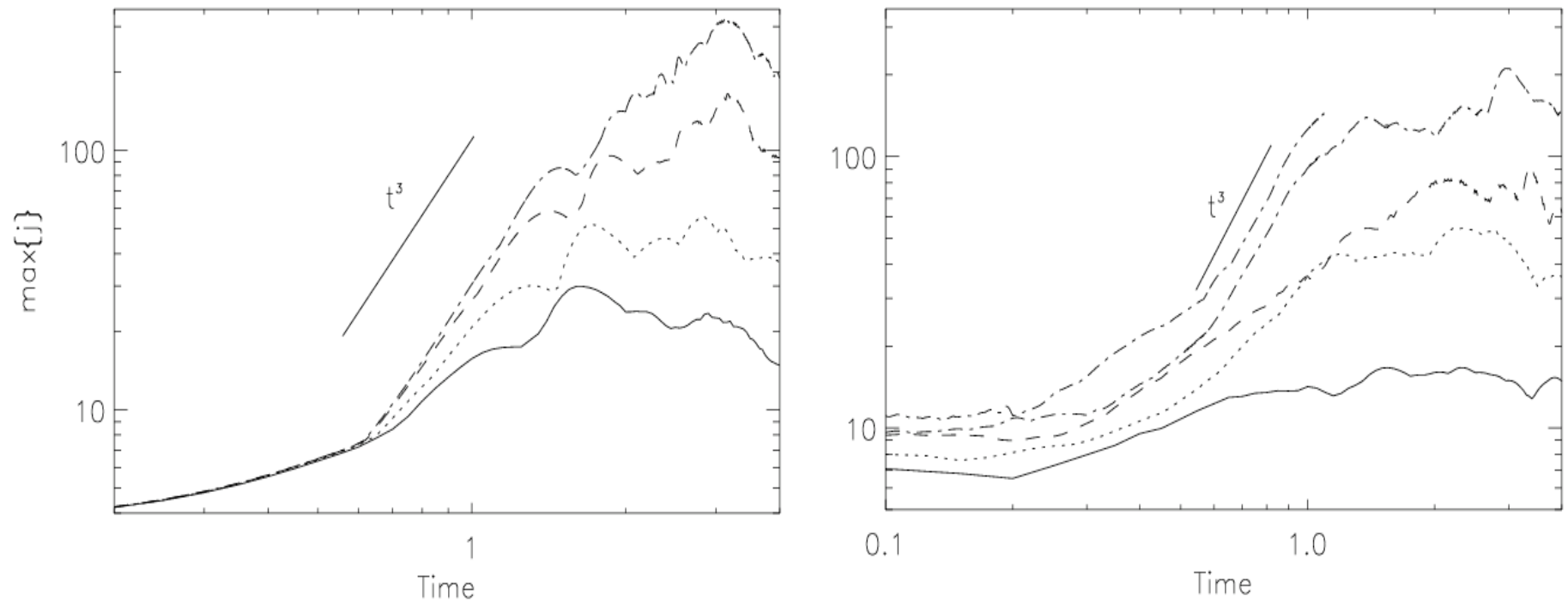
- The simulations with the Orszag-Tang vortex and random initial conditions show a self-similar growth of the current density as current sheets are formed. Then, the current sheets break down and saturation is reached.

- A 1536^3 MHD shows structures change at large Reynolds numbers

Lagrangian averaged MHD (α-model)

- The fields are written as the sum of filtered and fluctuating components

$$\mathbf{v} = \mathbf{u_s} + \delta\mathbf{v} \qquad \mathbf{v} = \left(1 - \alpha^2\nabla^2\right)\mathbf{u_s}$$

$$\mathbf{B} = \mathbf{B_s} + \delta\mathbf{B} \qquad \mathbf{B} = \left(1 - \alpha^2\nabla^2\right)\mathbf{B_s}$$

- The LAMHD equations are

$$\partial_t\mathbf{v} + \mathbf{u_s} \cdot \nabla\mathbf{v} + v_j\nabla u_s^j = -\nabla\mathcal{P} + \mathbf{j} \times \mathbf{B_s} - \nu\nabla \times \boldsymbol{\omega}$$
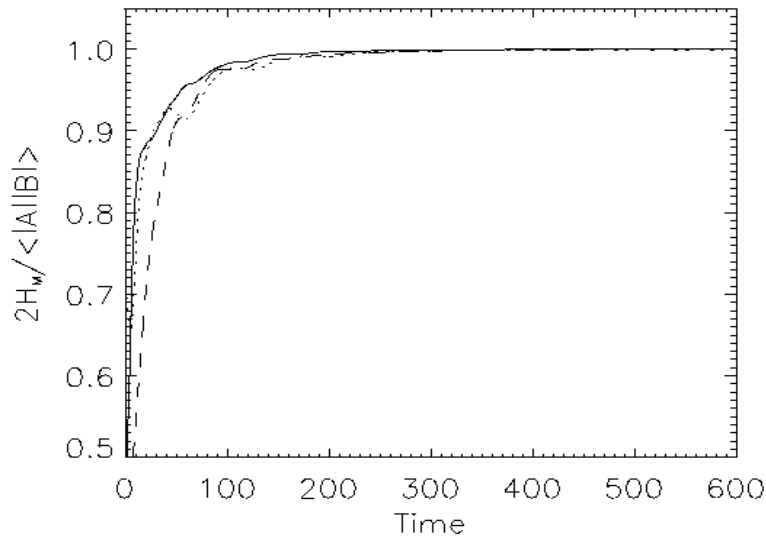
$$\partial_t\mathbf{B_s} + \mathbf{u_s} \cdot \nabla\mathbf{B_s} = \mathbf{B_s} \cdot \nabla\mathbf{u_s} - \eta\nabla \times \mathbf{j}$$

- The 3D invariants are $\quad E = \dfrac{1}{2}\displaystyle\int \left(\mathbf{u_s} \cdot \mathbf{v} + \mathbf{B} \cdot \mathbf{B_s}\right) \mathrm{d}^3x$

$$H_C = \frac{1}{2}\int \mathbf{v} \cdot \mathbf{B_s}\, \mathrm{d}^3x,$$

$$H_M = \frac{1}{2}\int \mathbf{A_s} \cdot \mathbf{B_s}\, \mathrm{d}^3x.$$

Holm, Chaos 12, 518 (2002);
Mininni, Montgomery, & Pouquet,
Phys. Fluids 1, 035112 (2005)

LAMHD: selective decay

- LAMHD was tested against four MHD problems: selective decay, dynamic alignment, inverse cascade, and dynamo action.

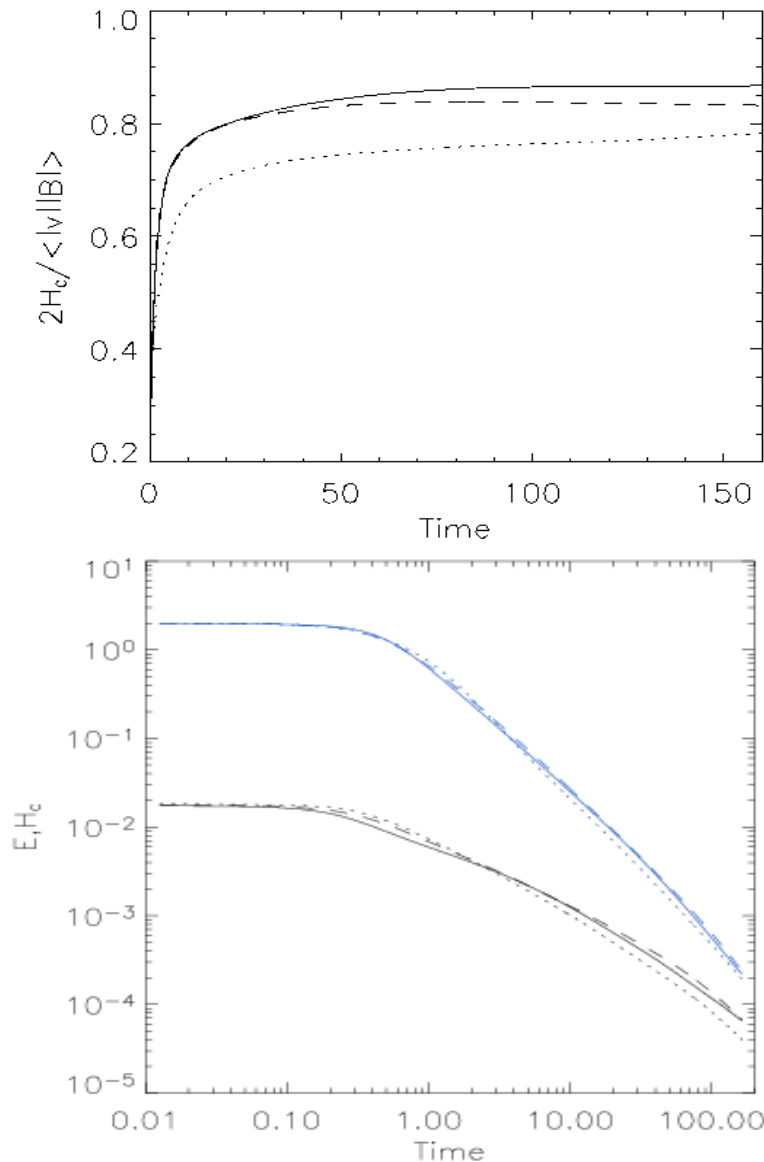- In selective decay, energy decays rapidly relative to magnetic helicity.

- Initial conditions:

$$\mathbf{v}(t=0) = \sum_{k=k_{\text{bot}}}^{k_{\text{top}}} v_0[\mathbf{v}_{ABC}(k,\phi_k) + \hat{\mathbf{v}}(\mathbf{k})e^{i\mathbf{k}\cdot\mathbf{x}}]$$

- $\mathbf{B}(t=0) = \sum_{k=k_{\text{bot}}}^{k_{\text{top}}} b_0[\mathbf{v}_{ABC}(k,\phi_k) + \hat{\mathbf{B}}(\mathbf{k})e^{i\mathbf{k}\cdot\mathbf{x}}]$

  decaying runs).

- 256^3 DNS [solid], 128^3 LAMHD ($\alpha_M = \alpha_V = 1/20$) [dashed], and 64^3 LAMHD ($\alpha_M = \alpha_V = 1/10$) [dotted].

Mininni, Montgomery, & Pouquet, PRE 71, 046304 (2005)
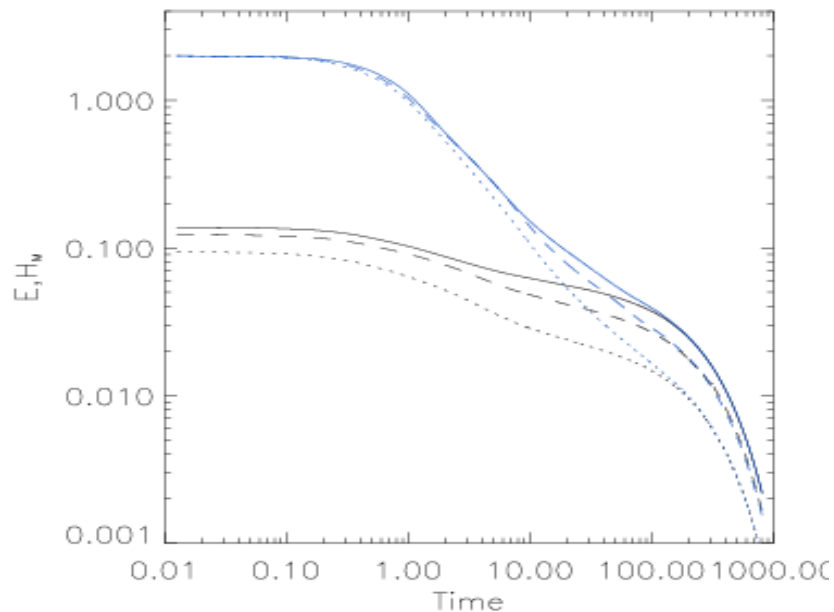
LAMHD: dynamic alignment

- In dynamic alignment, an initially small alignment between the magnetic and velocity fields is amplified as a function of time.

- The cross helicity decays slowly compared with the total energy.

- The alignment takes place mostly at small scales, a hard test for SGS models!

- In LAMHD, the SG stress tensor is symmetric in **v** and **B** (Alfven waves are solutions of LAMHD),

- To obtain dynamic alignment, we used: $k_{bot}=6$, $k_{top}=10$, $\eta=\nu=2\times10^{-3}$, $2H_c=0.3\langle|\mathbf{v}\|\mathbf{B}|\rangle$ (no helical component, free decaying runs).

- 256^3 DNS [solid], 128^3 LAMHD ($\alpha_M=\alpha_V=1/20$) [dashed], and 64^3 LAMHD ($\alpha_M=\alpha_V=1/10$) [dotted].

LAMHD: inverse cascades
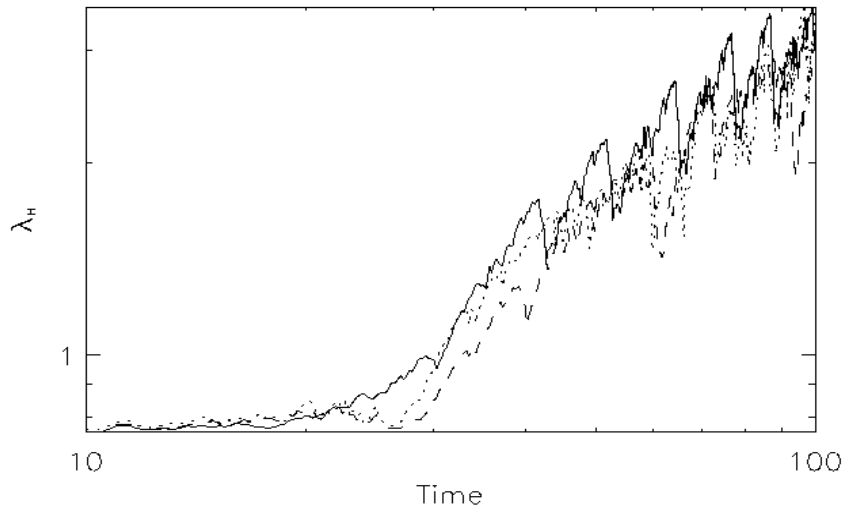
- In 3D MHD, magnetic helical excitations injected at small scales are transferred to large scales, creating coherent structures.
- A helical random electromotive force is applied in the Fourier ring $k=[8,9]$. Increase in the correlation length of **B** is observed, as well as an inverse cascade of H_M.
- 256^3 DNS [solid], 128^3 LAMHD ($\alpha_M=\alpha_V=1/20$) [dashed], and 64^3 LAMHD ($\alpha_M=\alpha_V=1/10$) [dotted].

(a) 256^3 DNS

(b) 128^3 LAMHD

(c) 64^3 LAMHD
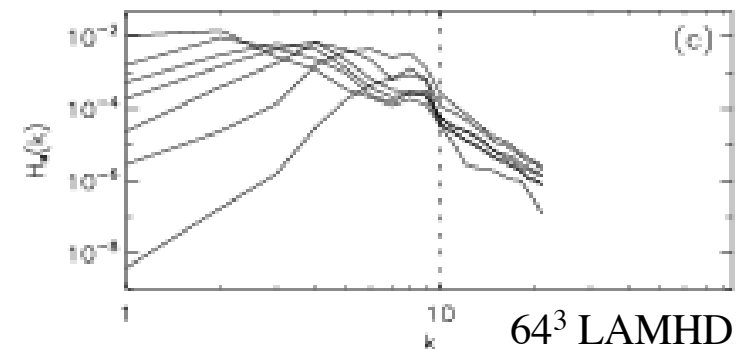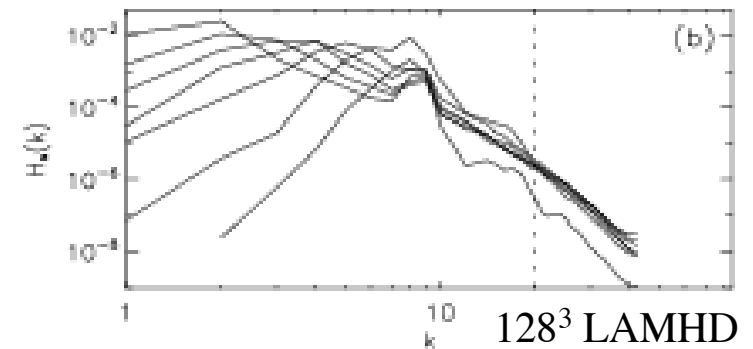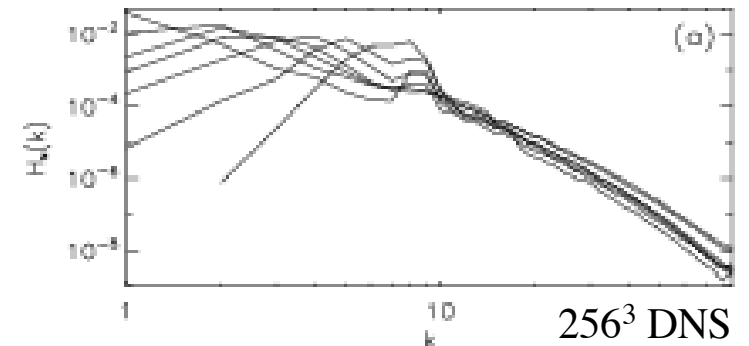
LAMHD: helical dynamo at $P_M=1$
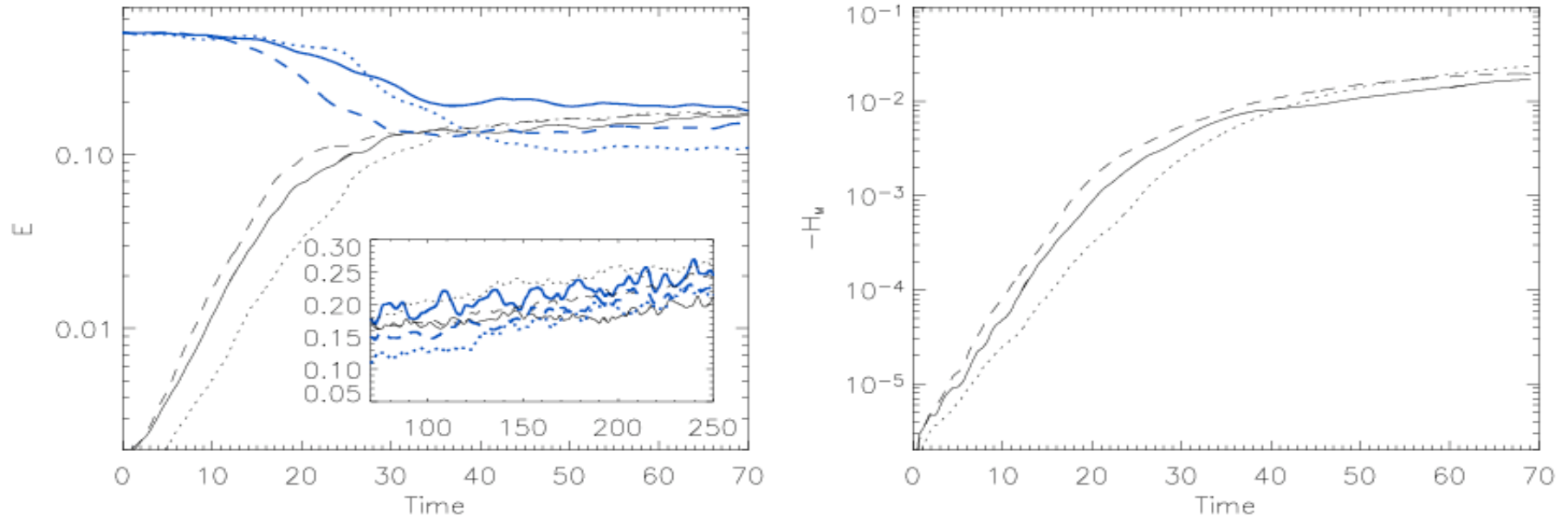
- A hydrodynamic simulation is done using a mechanic ABC forcing at $k=3$, until reaching a turbulent steady state.
- Then, a small magnetic seed is introduced, and the simulation is continued to observe exponential amplification of the magnetic field, and non-linear saturation ($\eta=\nu=2\times10^{-3}$).
- If the flow is helical, the magnetic field at large scales is helical and magnetic helicity grows with the opposite sign than the kinetic helicity.
- 256^3 DNS [solid], 128^3 LAMHD ($\alpha_M=\alpha_V=1/20$) [dashed], and 64^3 LAMHD ($\alpha_M=\alpha_V=1/10$) [dotted] (blue lines: kinetic energy; black lines: magnetic energy).

LAMHD: helical dynamo at $P_M=1$
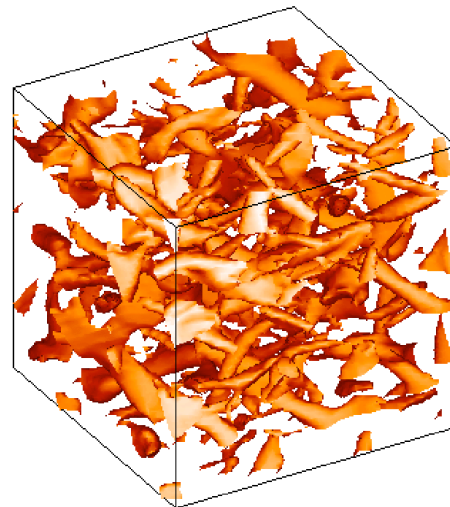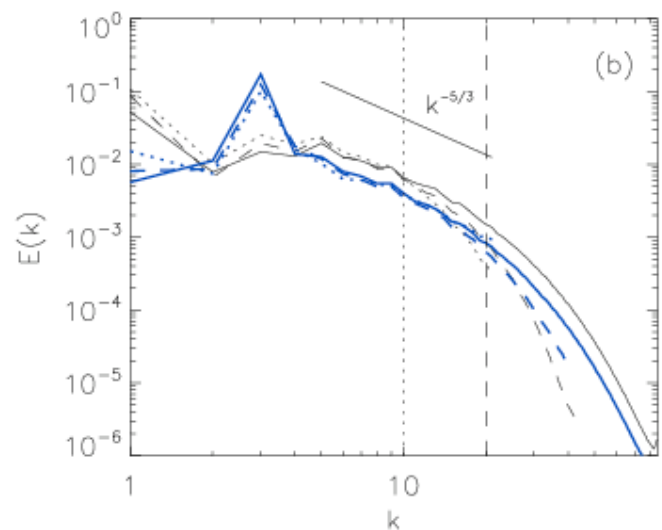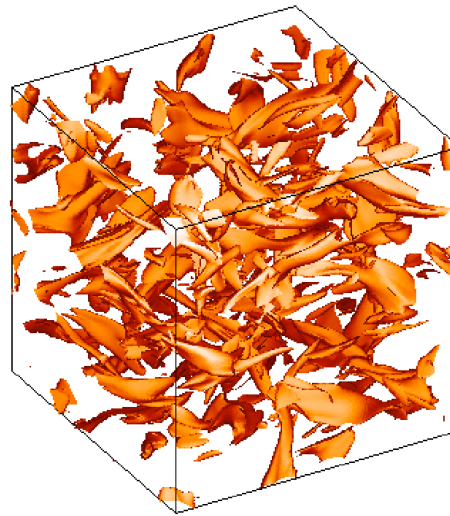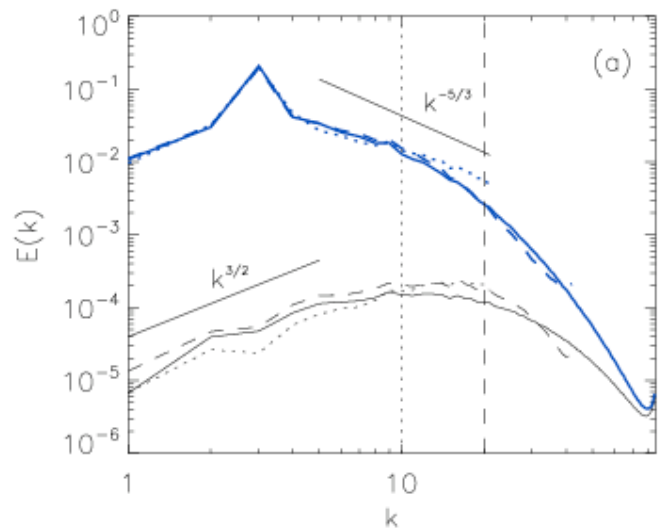
- The magnetic (black) and kinetic (blue) energy spectra are well captured, both in the kinematic regime and in the saturation.
- The model correctly captures the spectral behavior up to the wavenumner α^{-1}.
- Structures in LAMHD are thicker due to the introduction of the filtering length α.
- The tails in the PDFs are captured by the model (intermittency!).
- Intermittency can trigger large scale events, affect transport coefficients, or change the turbulent scaling.

Intermittency: results from simulations
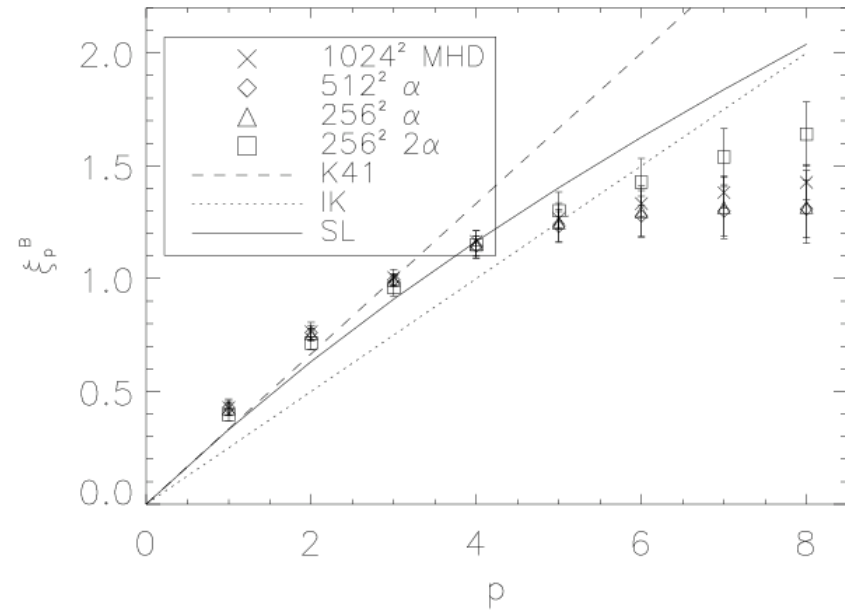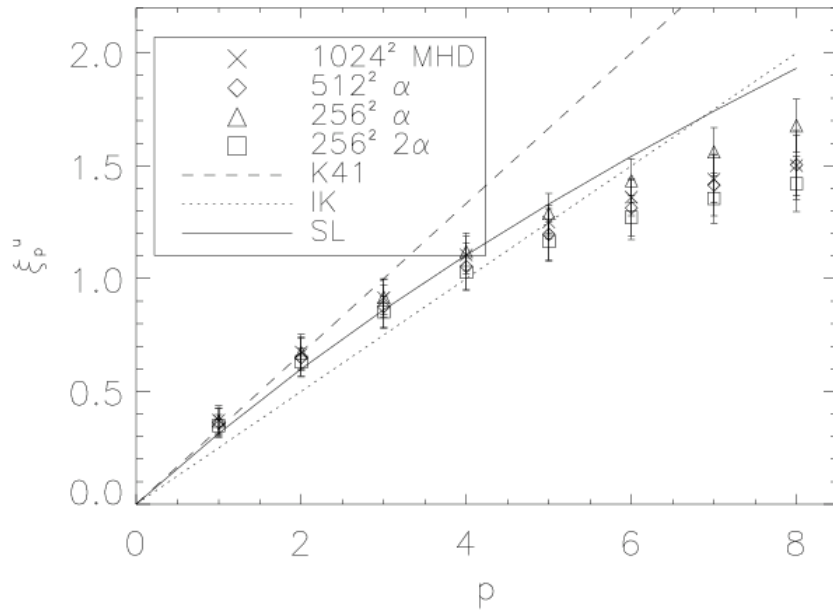
- 2D forced MHD simulations (1024^2 DNS, 512^2 LAMHD with $\alpha=1/80$, and two sets of 256^2 LAMHD with $\alpha=1/40$ and $\alpha=1/20$), 200 turnover times in each simulation, $\eta=\nu=1.6\times10^{-4}$.
- Random forcing, energy injected at large scales ($k=1,2$).
- Strong localized structures are characteristic of MHD turbulence and give rise to deviations from universality.
- The LAMHD equations capture high-order statistics (up to p=8), and the anomalous scaling of the longitudinal structure function exponents.

Conclusions

- A major problem of turbulence is to characterize the statistical properties of the flows.

- Progress can be made using a variety of techniques and contrasting them: theory, models, experiments, observations, and numerical simulations.

- We discussed results high-resolution DNS and models of three-dimensional Navier-Stokes and MHD turbulence, and posed several questions that may be relevant from a statistical point of view.

- These problems include:

- The problem of universality of statistical properties of turbulence, at either small or large scales. What is the PDF of the energy dissipation? What should we meassure to characterize structures in the flow?

- Parameter optimization. What is the optimal filtering scale in a LES?

- Model optimization. How do we decide between different LES models?